Journal of Chemical&Engineering Data

pubs.acs.org/jced

Article

pVT Data Analysis for the Prediction of Vapor Sorption in Glassy Polymers through the Nonequilibrium PC-SAFT Model

Ferruccio Doghieri*

Cite This: J. Chem. Eng. Data 2024, 69, 538−559

Read Online

ACCESS | Metrics & More | Article Recommendations | Supporting Information

ABSTRACT: The first implementation is presented for the Restrained Swelling (RS) version of the Nonequilibrium Thermodynamics for Glassy Polymers (NET-GP) approach, which counts on the PC-SAFT EoS to express the equilibrium properties of polymer-solute mixtures. Examples for application of the resulting model (NE-RS) PC-SAFT to the prediction of gas and vapor solubility in conventional glassy polymers are first discussed. Emphasis is put on the role of pVT properties for pure polymer species, as measured at both melt and glass conditions. The first application is then presented for the NE-RS approach to the analysis of gas and vapor solubility data in a polymer with intrinsic microporosity, for which pVT data in the melt phase cannot be measure and reliable values for the volumetric properties at glassy conditions are not available. In the latter analysis, both kinds of pVT properties are eventually retrieved from the best fit of the selected solubility data and the result for the polymer pVT characteristics are finally compared with those recently presented in the literature as obtained after the use of "Dry Glass Reference Perturbation Theory" (DGRPT), within the same NET-GP approach.

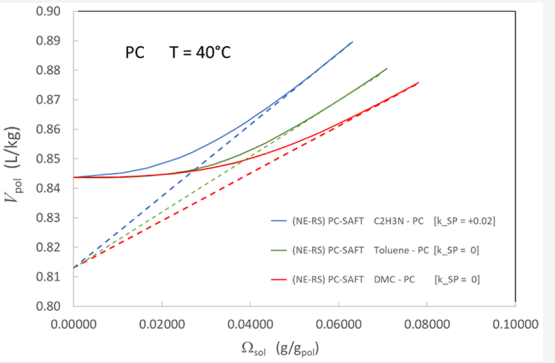

1. INTRODUCTION

Synthesis and formulation of new materials for the optimal design of gas separation membranes, as well as for the preparation of effective barrier films and coatings, largely benefit from capabilities of predictive tools for gas and vapor solubility in complex polymeric materials. Among the latter, particularly interesting are those tools which address the problem of representing the thermodynamic properties of glassy phases. On the side of materials and process engineering, the availability of models of this kind represents an opportunity, as both conventional polymeric glasses and new superglassy materials offer very interesting performances in terms of selectivity and solvent resistance.[1,2] On the side of thermodynamic research, the setup of these tools is a challenging topic, as the problem of representing nonequilibrium conditions in polymer-solute systems is still waiting for a fully satisfactory solution.

Different approaches have been proposed, in the past, to frame the representation of the properties of polymer glasses within the general laws of classical thermodynamics, offering different routes to the description of the out-of-equilibrium condition for glassy polymeric mixtures.[3−6] Among the simplest and most direct approaches is the the Nonequilibrium Thermodynamics of Glassy Polymers (NET-GP) approach, which is built after the assumption that the polymer mass density works as a proper order parameter for the representation of out-of-equilibrium conditions and by managing it in terms of an internal state variable for the system.[7] Once a valid expression is identified for the equilibrium Helmholtz free energy density, as a function of temperature and the mass densities of all components in the system, the solute chemical potential and the constant volume heat capacity can be estimated in the out-of-equilibrium state, from the NET-GP approach, provided independent pieces of information are available for the polymer mass density at the pseudoequilibrium conditions of interest.

The NET-GP approach was first applied to compressible lattice fluid theory by Sanchez and Lacombe,[8,9] leading to the "Nonequilibrium Lattice Fluid" (NE-LF) model,[10] but it was later linked to several EoS in the class of Perturbed-Hard-Spheres-Chain theories and in that of Statistical Associating Fluid Theories.[11] With respect to the case of simple application of the corresponding model for equilibrium properties, the need for information about pseudoequilibrium polymer density, in the NET-GP approach, calls for the additional characterization of the volumetric properties of the polymeric material of interest.

As an example, the problem of evaluation of the infinite dilution solubility coefficient S_0 for a gas in conventional glassy polymers can be mentioned. In this case, indeed, the equilibrium volumetric properties for a pure polymer above the glass transition temperature can be measured to retrieve single-component polymer EoS parameters, while direct measurement

Special Issue: In Honor of Gabriele Sadowski

Received: July 15, 2023
Revised: December 9, 2023
Accepted: December 11, 2023
Published: January 8, 2024

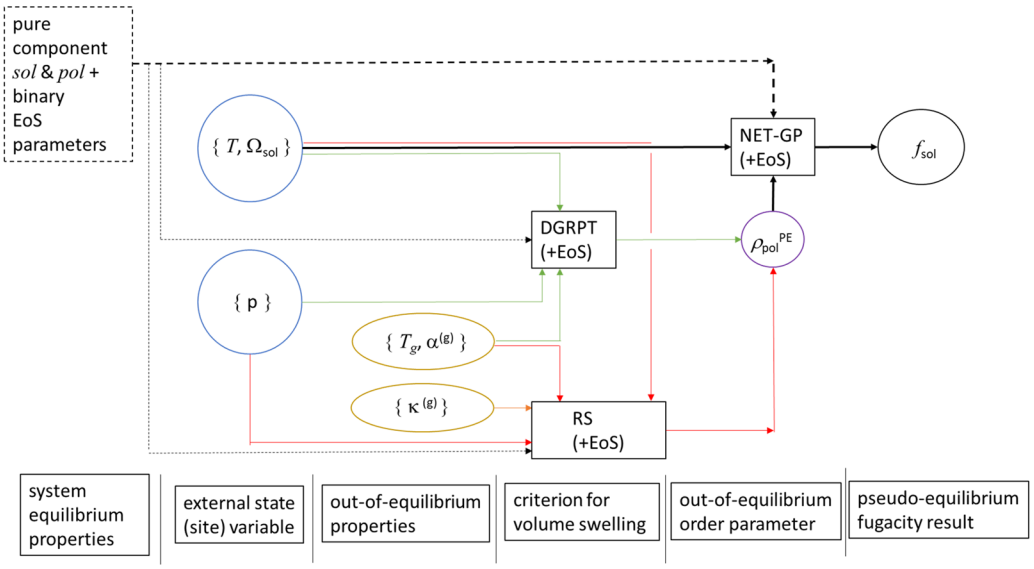

Figure 1. Representation of possible calculation paths for solute fugacity in a pseudoequilibrium solute-polymer glassy mixture.

of low-pressure dry polymer mass density, when accessible, can complete the set of variables required in the pertinent NET-GP procedure. Knowledge of S_0 is essential, for example, in the calculation of low-pressure gas permeabilities or barrier properties in polymers, and the NET-GP approach provides, indeed, a valuable and feasible route for its estimation in conventional glassy polymers.

On the other hand, the thermodynamic model which assists the analysis of materials to be evaluated to produce pervaporation or organic solvent nanofiltration membranes must have the capability of predicting high-activity vapor sorption. As for the use of the NET-GP model, the calculation route corresponding to the latter case would require information about the polymer mass density in a glassy swollen system. In this case, direct characterization of the polymer volume dilation induced by vapor sorption, as a function of the activity of all components, would be impractical, as well as challenging in technical terms. In fact, for a successful application of the NET-GP approach to the case of moderate-activity or high-activity vapor sorption in glassy polymers, a reliable criterion for pseudoequilibrium volume swelling needs to be integrated into the phase equilibrium problem for vapor solubility calculation.

In this respect, a few years ago we introduced the use of a criterion for the discussion of volume dilution induced by vapor sorption, which is based on a simplified model for bulk rheology of the solute-polymer glassy mixture.[12] We will hereafter refer to the model resulting from integration of this criterion into the NET-GP approach as the Nonequilibrium Restrained Swelling (NE-RS) model. The application of the latter relies on the knowledge of two out-of-equilibrium pure polymer parameters, as described in section 3 in the following.

An alternative criterion for sorption-induced volume swelling was recently introduced by Lively and co-workers,[13,14] based on an empirical thermodynamic approach, which directly links the sorption-induced swelling coefficient to the dry polymer density. In the model resulting from the integration of this latter criterion to the NET-GP approach, which is identified as "Dry Glass Reference Perturbation Theory" (DGRPT), the only out-of-equilibrium datum required for the solution of the pseudoequilibrium problem is the low-pressure polymer density at dry conditions. DGRPT closure of NET-GP approach results are appealing, in view of its relatively simple structure and of the possibility to run the calculation of solubility at high vapor activity accounting for knowledge of the same out-of-equilibrium property which is required for the evaluation of the infinite dilution solubility coefficient.[15]

Numerous calculations and comparisons with experimental data of the results from DGRPT, provided in recent publications, prove that the empirical thermodynamic approach used by Lively and co-workers captures several characteristics of the phenomenon underlying the swelling of a polymeric mixture below the glass transition temperature.[16] On the other hand, it should be noted that most examples discussed through the application of the DGRPT model refer to the case of "superglassy polymers", corresponding to materials whose extremely high glass transition prevents the possibility to directly measure pure polymer equilibrium volumetric properties for the tuning of EoS parameters. In the application of the DGRPT model, then, all equilibrium and nonequilibrium parameters are typically retrieved from the best fit of pseudoequilibrium solubility data, at both low and high pressure.

The limited number of applications of DGRPT to cases in which model parameters can be independently retrieved with respect to solubility data did not allow, so far, challenge of the proposed link between dry polymer properties and vapor−liquid equilibria. The latter would also be useful to discuss what appears as a limit of the model, for which the nonequilibrium swelling behavior is univocally identified by the dry polymer mass density. It is well-known, in fact, that the swelling behavior of glassy polymers may be different, according to the preparation protocol and conditioning treatment, even when the dry polymer density does not significantly depart from the case of the standard glass phase. The representation of this complex behavior, instead, may be attempted using the NE-RS model, in which the pseudoequilibrium behavior is interpreted based on two distinct out-of-order parameters.[17,18]

Possible routes for the NET-GP calculation of solute fugacity in a glassy solute-polymer mixture, at assigned temperature T, pressure p, and solute mass ratio Ω_{sol}, are schematically represented also in Figure 1. Black lines in the figure refer to the use of the nonequilibrium thermodynamic approach for the peculiar case in which direct, independent information is

https://doi.org/10.1021/acs.jced.3c00441
J. Chem. Eng. Data 2024, 69, 538−559

available for the out-of-equilibrium polymer density ρ_{pol}^{PE} in the swollen glassy system. Red lines and green lines, in the same figure, schematically illustrate the calculation paths for the polymer density in the pseudoequilibrium swollen glassy system as depicted by the NE-RS and DGRPT models, respectively. The plot puts in evidence the distinct sets of out-of-equilibrium properties the two models account for, in the estimation of ρ_{pol}^{PE}.

The flowchart shown in Figure 1 also emphasizes the role of the general equilibrium and nonequilibrium pVT properties of the system, as well as that of external variables ("site" variables in rational thermodynamics terms[19]) and out-of- equilibrium order parameters ("internal state" variables in the same scheme[19]).

The direct comparison of the capability and performance of the alternative routes described above for the calculation of the solubility of low-molecular-weight species in glassy polymer, within the NET-GP approach, is not the scope of this work. We rather aim here at recognizing similarities and differences between volume dilation behavior at sorption condition, as returned by the application of the two different routes. To this aim, it is here considered, for the first time, the application of the NE-RS model to the analysis of gas and vapor sorption in a superglassy polymer.

The case of a polymer with intrinsic microporosity (PIM-1) is considered for this purpose, whose examination was also addressed in the work by Marshall on the application of DGRPT.[20] The set of equilibrium and nonequilibrium pVT properties of pure PIM-1, for which experimental data are not available, is here retrieved from the best fit of selected experimental data for vapor solubility in the glassy polymer. The properties retrieved this way are then used to predict the solubility isotherms for more components in the glassy matrix. The same pVT properties will be finally compared with those derived from the use of DGRT, and the general characteristics of the sorption-induced volume dilation predicted by the two models will be discussed.

In consideration of its versatility and of the success reached in the last 20 years, PC-SAFT, introduced by Prof. Sadowski,[22,22] is here used as the EoS for the representation of equilibrium thermodynamic properties. To emphasize the role of the model parameters in the NET-GP and NE-RS models, the analysis of low-pressure gas solubility and high-activity vapor solubility data in a conventional glassy polymer will be here considered first, with specific attention to the procedure for retrieval of model parameters from pure component pVT properties, for both equilibrium and nonequilibrium conditions.

2. NET-GP AND (NE) PC-SAFT

After the choice of polymer mass density as the out-of-equilibrium order parameter, and through the use of tools from the thermodynamics of systems endowed with internal state variables,[19] the following conclusions are finally drawn, in the original NET-GP approach, to the description of binary solute-polymer mixtures:[10] (a) at pseudoequilibrium conditions for the system, the pressure generally departs from the negative of the derivative of the Helmholtz free energy with respect to the system volume at constant temperature, mass, and composition, while (b) the solute chemical potential can still be calculated after the derivative of the Helmholtz free energy with respect to solute content, at constant temperature, volume, and polymer mass. In view of the above conclusions, the pseudoequilibrium solute fugacity f_{sol}^{PE} is calculated, as a function of temperature T and set of species concentrations (ρ_{solb} ρ_{pol}), from the very same expression which holds at equilibrium, with the peculiar condition that the volume of the mixture per polymer mass $V_{pol} = 1/\rho_{pol}$ cannot be calculated after the equation of state for pressure, but it needs to be input to the problem from independent information about the actual pseudoequilibrium value of the polymer mass density $\overline{\rho_{pol}}^{PE}$:

$$\begin{cases} f_{sol}{}^{PE} = f_{sol}{}^{EQ}(T, \rho_{sol}, \rho_{pol}) \\ \rho_{pol} = \overline{\rho_{pol}}^{PE} \end{cases} \tag{2.1}$$

For the objective of this work, it is important to observe that the solubility coefficient $S_{sol}(T, p, \Omega_{sol})$ of the solute species in the solute-polymer mixture, at assigned temperature T, pressure p, and solute mass ratio Ω_{sol}, defined as

$$S_{sol}(T, p, \Omega_{sol}) = \left[\left(\frac{\partial f_{sol}}{\partial \rho_{sol}}\right)_{T,p}\right]^{-1} \tag{2.2}$$

depends on both polymer density ρ_{pol} and swelling coefficient κ_Ω in the mixture, which, in turn, is here defined by the following relation

$$\kappa_\Omega = +\frac{1}{V_{pol}}\left(\frac{\partial V_{pol}}{\partial \Omega_{sol}}\right)_{T,p} = -\frac{1}{\rho_{pol}}\left(\frac{\partial \rho_{pol}}{\partial \Omega_{sol}}\right)_{T,p} \tag{2.3}$$

Indeed, accounting for eq 2.1, the derivative which defines S_{sol} can be detailed as indicated in eq 2.4:

$$\left(\frac{\partial f_{sol}}{\partial \rho_{sol}}\right)_{T,p} = \left(\frac{\partial f_{sol}^{EQ}}{\partial \rho_{sol}}\right)_{T,\rho_{pol}} + \left(\frac{\partial f_{sol}^{EQ}}{\partial \rho_{pol}}\right)_{T,\rho_{sol}}\left(\frac{\partial \rho_{pol}}{\partial \rho_{sol}}\right)_{T,p} \tag{2.4}$$

and when the following general relation is accounted for

$$\left(\frac{\partial \rho_{sol}}{\partial \rho_{pol}}\right)_{T,p} = \left(\frac{\partial(\Omega_{sol}\rho_{pol})}{\partial \rho_{pol}}\right)_{T,p} = \Omega_{sol} + \rho_{pol}\left(\frac{\partial \Omega_{sol}}{\partial \rho_{pol}}\right)_{T,p} \tag{2.5}$$

the conclusion in eq 2.6 can be finally drawn:

$$S_{sol}(T, p, \Omega_{sol}) = \frac{1}{\left(\frac{\partial f_{sol}^{EQ}}{\partial \rho_{sol}}\right)_{T,\rho_{pol}} + \left(\frac{\partial f_{sol}^{EQ}}{\partial \rho_{pol}}\right)_{T,\rho_{sol}}\frac{\kappa_\Omega}{\kappa_\Omega\Omega_{sol} - 1}} \tag{2.6}$$

from which the effect of κ_Ω on S_{sol} is in evidence. If the attention is confined to the low-pressure, infinite dilution coefficient $S_{0,sol} = S_{sol}(T, p \to 0, \Omega_{sol} \to 0)$, it must be considered that, in this limit, the equilibrium solute fugacity function returns to zero, irrespective of the value of polymer density ρ_{pol}, so that $\lim_{\Omega_{sol}\to 0}\left(\frac{\partial f_{sol}^{EQ}}{\partial \rho_{pol}}\right)_{T,\rho_{sol}} = 0$ at all temperature and pressure, and finally

$$\begin{aligned} S_{0,sol}(T) &= \left[\lim_{\substack{\rho_{sol}\to 0 \\ p\to 0}}\left(\frac{\partial f_{sol}^{EQ}}{\partial \rho_{sol}}\right)_{T,\rho_{pol}}\right]^{-1} \\ &= \lim_{\substack{\rho_{sol}\to 0 \\ p\to 0}}\left(\frac{\rho_{sol}}{f_{sol}^{EQ}(T, \rho_{sol}, \rho_{pol})}\right) \end{aligned} \tag{2.7}$$

The above equation reveals that the infinite dilution solubility coefficient $S_{0,sol}$ at assigned temperature T depends on the

https://doi.org/10.1021/acs.jced.3c00441
J. Chem. Eng. Data 2024, 69, 538−559

corresponding value of the dry polymer density ρ_{pol}^{0}, which, in turn, corresponds to the low-pressure equilibrium pure polymer density at T, for the case $T > T_g$, and to the pertinent pseudoequilibrium value in the opposite case.

For the case of glassy states, the pseudoequilibrium dry polymer density $\rho_{pol}^{0,PE}$ needs to be specifically evaluated for the temperature of interest, according to the preparation protocol used:

$$\begin{cases} S_{0,sol}(T) = \lim_{\rho_{sol}\to 0} \dfrac{\rho_{sol}}{f_{sol}^{EQ}(T, \rho_{sol}, \rho_{pol})} \\ \rho_{pol} = \rho_{pol}^{0,PE}(T) \end{cases} \tag{2.8}$$

For the case in which glassy polymer samples are prepared from the melt phase, after standard cooling protocols, the pseudoequilibrium polymer density $\rho_{pol}^{0,PE}$ is calculated from the information about the low-pressure glass transition temperature T_g and standard glassy thermal expansion coefficient $\alpha^{(g)}$:

$$\begin{cases} S_{0,sol}(T) = \lim_{\rho_{sol}\to 0} \dfrac{\rho_{sol}}{f_{sol}^{EQ}(T, \rho_{sol}, \rho_{pol})} \\ \rho_{pol} = \rho_{pol,g}\exp[\alpha^{(g)}(T_g - T)] \\ p' = p^{EQ}(T_g, \rho_{sol} = 0, \rho_{pol,g}) \end{cases} \tag{2.9}$$

where $p^{EQ}(T, \rho_{sol}, \rho_{pol})$ is the equilibrium pressure function in the mixture at the assigned temperature and species density and p' is a conveniently low positive value for pressure.

The latter set of equation should be compared with that pertinent to the corresponding true thermodynamic equilibrium problem:

$$\begin{cases} S_{0,sol}(T) = \lim_{\rho_{sol}\to 0} \dfrac{\rho_{sol}}{f_{sol}^{EQ}(T, \rho_{sol}, \rho_{pol})} \\ p' = p^{EQ}(T, \rho_{sol} = 0, \rho_{pol}) \end{cases} \tag{2.10}$$

where the expressions $p^{EQ}(T, \rho_{sol}, \rho_{pol})$ and p' are used with the same meaning indicated above.

When PC-SAFT is used to represent the equilibrium properties of nonassociating solute-polymer mixtures, f_{sol}^{EQ} is expressed in terms of the following parameters: Boltzmann constant k, solute and polymer molecular mass M_s and M_p, hard sphere diameter σ_s and σ_p, number of hard spheres per molecule m_s and m_p, characteristic interaction energy ε_s and ε_p, as well as solute-polymer binary interaction parameter k_{sp}, which interprets the nonhomogeneous interaction energy ε_{sp} according to the following expression:

$$\varepsilon_{sp} = (1 - k_{sp})\sqrt{\varepsilon_p}\sqrt{\varepsilon_s} \tag{2.11}$$

In the present analysis, however, all calculations will be referred to the limiting case of infinite molecular mass for the polymer species ($M_p \to \infty$), so that the list of parameters reduces as indicated hereafter

$$f_{sol}^{EQ} = f_{sol}^{EQ}(T, \rho_{sol}, \rho_{pol}; k, M_s, \sigma_s, \sigma_p, M_s/m_s, M_p/m_p, (\varepsilon/k)_s, (\varepsilon/k)_p, k_{sp}) \tag{2.12}$$

According to the NET-GP model, in the moderate-to-high pressure range, the pseudoequilibrium solute content ρ_{sol}^{PE} in the polymer solute-mixture which is in contact with a pure solute gas phase (G) at assigned pressure p and temperature T is obtained through the solution of the following set of equations:

$$\begin{cases} f_{sol} = f_{sol}^{(G)}(T, p) \\ f_{sol} = f_{sol}^{EQ}(T, \rho_{sol}^{PE}, \rho_{pol}) \\ \rho_{pol} = \overline{\rho_{pol}}^{PE} \end{cases} \tag{2.13}$$

in which $f_{sol}^{(G)}$ is the expression for the fugacity of a pure solute gas phase. To close the above mathematical problem for the evaluation of ρ_{sol}^{PE} at the assigned T and p, the pseudoequilibrium polymer density $\overline{\rho_{pol}}^{PE}$ corresponding to the pressure value and solute content of interest needs to be input from specific, independent information, or its relation to the set of variables T, p, and ρ_{sol} needs to be provided.

3. NET GP WITH RESTRAINED SWELLING MODEL [(NE-RS) PC-SAFT]

A closure for the problem addressed by the set of eqs 2.13 is proposed in the NE-RS model,[17] interpreting the bulk rheological behavior below T_g through a simple model, which combines two Voigt elements in series, the first one being characterized by a very large characteristic time ("hard element"), while the second one is characterized by a very short characteristic time ("soft element"). In this simplified picture, the volume of the hard element is frozen, while that of the soft element corresponds to the equilibrium value for pertinent temperature, pressure, and solute fugacity. The relative weight χ the elements contribute to the overall specific polymer volume corresponds to the ratio between the isothermal compressibility below and above the glass transition temperature:

$$\chi = \frac{\kappa^{(g)}}{\kappa^{(m)}} = \frac{(\partial\rho^{PE}/\partial p)_{g-}}{(\partial\rho^{EQ}/\partial p)_{g+}} \tag{3.1}$$

The overall phase equilibrium problem (under pseudoequilibrium conditions) is finally summarized in the following set of equations:[12]

$$\begin{cases} f_{sol} = f_{sol}^{(G)}(T, p) \\ f_{sol} = f_{sol}^{EQ}(T, \rho_{sol}^{PE}, \rho_{pol}) \\ \rho_{pol}^{0,PE}(T, p) = \rho_{pol}^{0,EQ}(T_g, p)[\alpha^{(g)}(T_g - T)] \\ \dfrac{1}{\rho_{pol}^{PE}} = \dfrac{1}{\rho_{pol}^{0,PE}(T, P)} + \chi\left(\dfrac{1}{\rho_{pol}^{EQ}(T, f_{sol}, p)} - \dfrac{1}{\rho_{pol}^{0,EQ}(T, p)}\right) \end{cases} \tag{3.2}$$

In the above set of equations, $\rho_{pol}^{0,EQ}$ and ρ_{pol}^{EQ} are functions for the equilibrium polymer density in the pure polymer and in the solute-polymer mixture, respectively.

In the following sections, analysis will be performed of pseudoequilibrium solubility data in glassy polymers, using the NET-GP approach applied to the PC-SAFT equation of state, to discuss the infinite dilution gas solubility, for which volume swelling information is not required [(eq 2.9), (NE) PC-SAFT model], while the corresponding Nonequilibrium Restrained Swelling model [(eq 3.2), (NE-RS) PC-SAFT model] will be used for the analysis of vapor solubility in the moderate-to-high

https://doi.org/10.1021/acs.jced.3c00441
J. Chem. Eng. Data 2024, 69, 538−559

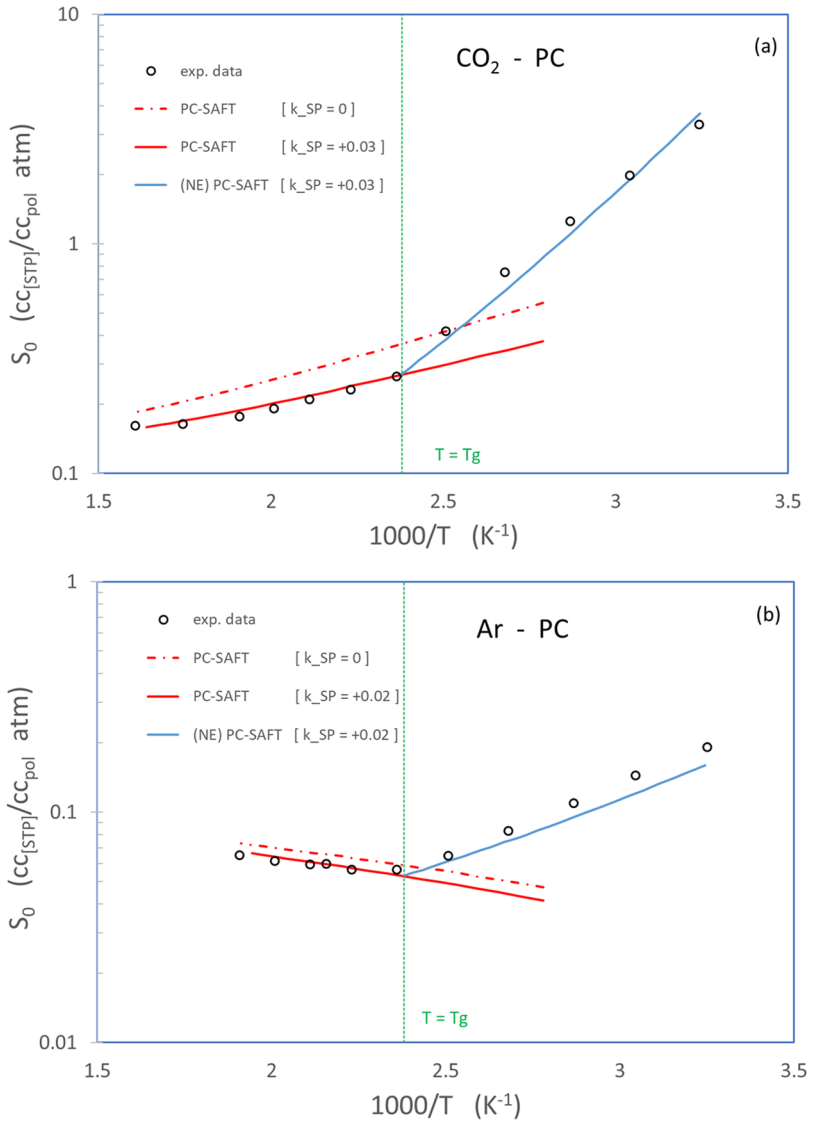

Figure 2. Analysis of infinite dilution gas solubility coefficient in PC: (a) CO_2, experimental data from ref 20; (b) Ar, experimental data from ref 20.

activity range. Attention will be focused also on the problem of retrieving equilibrium EoS parameters and nonequilibrium volumetric properties in the procedure.

4. ANALYSIS OF GAS/VAPOR SOLUBILITY IN POLYCARBONATE

4.1. Infinite Dilution Gas Solubility Coefficient in Polycarbonate (PC). The use of the PC-SAFT EoS for the analysis of solubility in glassy polymers is first illustrated considering experimental data available in the literature, pertinent to the infinite dilution solubility coefficient S_0 for Ar and CO_2 in PC. Experimental data for S_0 as a function of temperature, measured by Kamiya and co-workers,[23] are reported, in symbols, in Figure 2a (CO_2) and Figure 2b (Ar). Data clearly exhibit distinct trends in the temperature ranges above and below the glass transition point for PC (T_g = 147 °C), and rather different values can be calculated for the infinite dilution sorption enthalpy $\Delta\tilde{H}_{0,sol}$ in the two temperature ranges, according to the van't Hoff equation:

$$\Delta\tilde{H}_{0,sol} = -R\frac{d\ln S_{0,sol}}{d(1/T)} \tag{4.1}$$

Before considering the different values measured for S_0 and for $\Delta\tilde{H}_{0,sol}$ above and below the glass transition point, it should be clarified that data have different significance in the two regions. Experimental data retrieved in the melt phase, indeed, are representative of true equilibrium thermodynamic conditions and are univocal for the binary system of interest, at the assigned temperature. On the other hand, data measured in the glassy state correspond to pseudoequilibrium conditions reached after specific preparation protocols, and the results vary according to the procedure used. As a matter of fact, while we can refer to values for S_0 reported in ref 24 as pertinent to PC samples produced by standard cooling protocols from the melt phase, different results should be expected, at the same temperature for the case of annealed or preswollen samples.[18]

As for the analysis of experimental data measured by Kamiya, it can be observed that above the glass transition temperature, CO_2 exhibits a negative value for the enthalpy of sorption in PC (corresponding to an exothermic sorption process) equal to $\Delta\tilde{H}_{0,sol} = -4.3$ *kJ/mol K*, while a positive value (endothermic process) equal to $\Delta\tilde{H}_{0,sol} = +3.0$ *kJ/mol K* is registered for Ar in the same temperature range. On the other hand, significantly higher negative values of enthalpy of sorption are measured for

https://doi.org/10.1021/acs.jced.3c00441
J. Chem. Eng. Data 2024, 69, 538−559

Table 1. PC-SAFT Parameters for Gas, Vapors, and Polymers, Used in Solubility Calculations

substance	M (g/mol)	ε/k (K)	σ ($Å$)	m/M (g/mol)	ref	source of exp data
N_2	28.010	90.96	3.3130	0.04304	21	
O_2	32.000	114.96	3.2100	0.03505	21	
Ar	39.948	122.23	3.4784	0.02324	21	
CO_2	44.000	169.21	2.7852	0.04711	21	
CH_4	16.040	150.03	3.7039	0.06246	21	
C_2H_4	28.050	176.47	3.4450	0.05679	21	
C_2H_6	30.070	191.42	3.5206	0.05344	21	
C_3H_6	42.080	207.19	3.5356	0.04657	21	
C_3H_8	44.090	208.11	3.6184	0.04540	21	
n-heptane	100.200	238.40	3.8049	0.03476	21	
Toluene	92.140	285.69	3.7169	0.03055	21	
Acetonitrile	41.050	311.31	3.1898	0.05674	39	
DMC	90.080	240.00	3.1000	0.04167	this work	27
Methanol[a]	32.040	225.00	2.3500	0.12500	this work	28
Ethanol[a]	46.069	198.24	3.1771	0.12500	this work	28
Water[a]	18.020	335.00	2.0900	0.14925	this work	28
PC	∞	275.00	3.0630	0.04100	this work	25
PIM-1	∞	185.00	3.0000	0.03300	this work	(−)

[a]Nonassociating model.

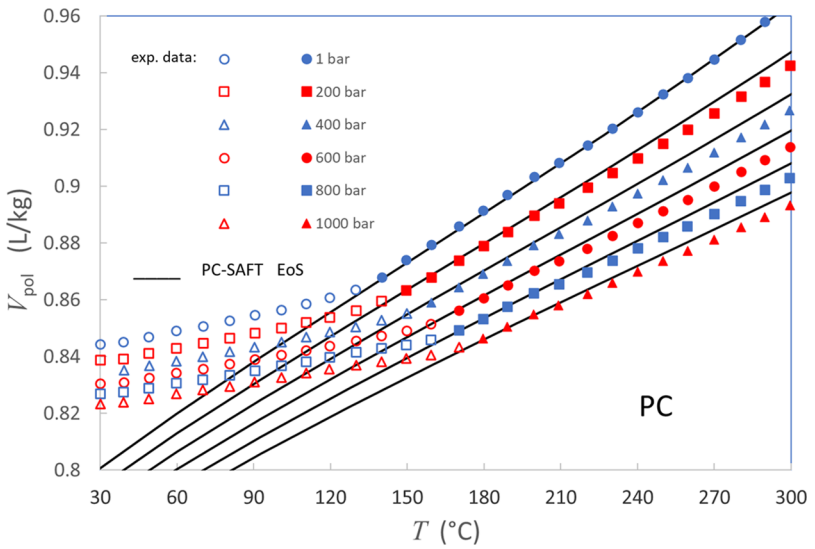

Figure 3. Specific volume of PC as a function of temperature and pressure [exp data from ref 25].

both Ar ($\Delta\tilde{H}_{0,sol} = -12\ kJ/mol\ K$) and CO_2 ($\Delta\tilde{H}_{0,sol} = -24\ kJ/mol\ K$) below the glass transition point. This is a typical result for infinite dilution gas solubility in polymers, for which the nature of the gas sorption process in the glassy state is invariably exothermic and the heat of sorption is often an order of magnitude larger than the value measured for the melt phase.

To interpret the solubility coefficient through the EoS model, the retrieval of pure component parameters is in order. As it refers to low-molecular-weight species, PC-SAFT parameters, including hard sphere diameter σ, characteristic energy ε, and number of spheres per molecule m, were retrieved from the literature and listed in Table 1, together with molecular mass M. It should be noted that they are typically determined through the best fit of vapor pressure and saturated liquid density data. Because of that, the procedure to retrieve pure component PC-SAFT parameters for vapor species indeed allows accounting for experimental data in temperature ranges including room conditions, which are often of interest in solubility calculations.

For the case of permanent gases, instead, there is typically a significant gap between temperature values at which the parameters are retrieved and those at which they are used in predictive solubility calculations. The latter observation also applies to polymeric species in the calculation of interest in this work, for which equilibrium pVT data, when available, are pertinent to the temperature range above the glass transition point, while target conditions in the calculation obviously lie below. It should be finally mentioned that, for PC-SAFT, it is typically suggested binary VLE or LLE results are included in the set of experimental data to be used for the retrieval of pure component polymer parameters.[24] In this work, however, to stress the significance of pure polymer characteristics in the procedure, only pure component data will be accounted for, in determining pure polymer PC-SAFT parameters, and specific attention will be given to experimental data measured at the lowest possible temperature (corresponding to the glass transition point T_g). Finally, it is necessary to specify that all

https://doi.org/10.1021/acs.jced.3c00441
J. Chem. Eng. Data 2024, 69, 538−559

calculations are here performed in the limit of infinite value of molecular mass of the polymeric species, which is indeed definitely acceptable in volumetric properties or solubility calculations, when the actual average molecular mass exceeds 10^4 *kg/kmol*.

Under this assumption, for the case of nonassociating polymeric species, three model parameters need to be determined and, for the reason mentioned above, experimental data for three independent equilibrium pVT properties at the glass transition ($T = T_g^+$, melt phase) will be considered: low-pressure mass density, isothermal compressibility, and thermal expansion coefficient $\{T_g, \rho_{Tg}, \kappa_{Tg}^{(m)}, \alpha_{Tg}^{(m)}\}$. Experimental pVT data for amorphous PC, above and below the glass transition temperature, are reported in Figure 3 as measured by Zoller,[25] and they can be used to estimate the above values of properties of interest: $T_g = 147\ K$; $\rho_{Tg} = 1.16\ kg/L$; $\kappa_{Tg}^{(m)} = 5.8 \times 10^{-4}\ MPa^{-1}$ and $\alpha_{Tg}^{(m)} = 6.7 \times 10^{-4}\ K^{-1}$.

The set of experimental data $\{T_g, \rho_{Tg}, \kappa_{Tg}^{(m)}, \alpha_{Tg}^{(m)}\}$ may be used directly to retrieve PC-SAFT EoS parameters through a straightforward procedure described in the Supporting Information. Results for hard sphere mass, diameter, and characteristic energy for PC have been here obtained from its application, and corresponding values are reported in Table 1. Results for the model description of equilibrium volume are compared with experimental data in Figure 3, in the temperature range from room conditions to 300 °C and for pressures up to 1000 bar. It can then be noted that the model, set up on the basis of melt volumetric properties at the low-pressure glass transition point, indeed allows for a satisfactory representation of volumetric behavior in a large temperature and pressure range above T_g, while experimental results for specific volume at lower temperature invariably lie above the corresponding equilibrium value calculated through the PC-SAFT EoS. The positive difference between experimental pseudoequilibrium specific volume and calculated equilibrium value below T_g can be regarded as a measure of the "excess free volume", characteristic of dry polymer glassy phase, which is ultimately responsible for the enhancement in gas solubility coefficient, with respect to the melt phase.

Calculation of the equilibrium infinite dilution solubility coefficient is first in order, and indeed, results from solution of the corresponding true thermodynamic equilibrium problem [eq 2.10] are reported in red lines in Figure 2. In dash-and-point lines, results are reported for the case of the default value of the binary interaction coefficient ($k_{sp} = 0$), while solid red lines show the result of the best fit of the equilibrium solubility coefficients above the glass transition temperature, obtained by adjusting k_{sp} values. It can be observed that values of the enthalpy of sorption above T_g are already correctly represented by PC-SAFT, when null k_{sp} values are considered in the calculation, both for the case of the endothermic equilibrium sorption process (Ar) and for the exothermic case (CO_2). In addition, it should be observed that only modest adjustments of the binary interaction parameter are required to allow for an excellent representation of experimental data above the glass transition temperature, for both gases.

A simplified schematic of the numerical algorithm for the solution of the phase equilibrium problem in eq 2.10, as well as for the others of interest in this work, is offered in the Supporting Information which accompanies this paper.

After temperature-independent optimal binary interaction parameter values are identified for both Ar-PC and CO_2-PC pairs, the calculation of the infinite dilution solubility coefficient below the glass transition temperature can be performed according to the (NE) PC-SAFT problem in eq 2.9, after the value of the thermal expansion coefficient $\alpha_{Tg}^{(g)}$ for polycarbonate is accounted for. The latter datum is again read from the experimental data shown in Figure 3, and it is reported in Table 2.

Table 2. Nonequilibrium Parameters for Polymers, Used in Solubility Calculations

substance	T_g (K)	$\alpha^{(g)}$ (K^{-1})	χ (−)	ref	source of exp data
PC	420	2.0×10^{-4}	0.69	this work	25
PIM-1	643	2.0×10^{-4}	0.90	this work	(−)

The results for S_0, obtained from the solution of the problem in eq 2.9, are shown in blue lines in the plots represented in Figure 2. It can be appreciated that the considerable enhancement in solubility coefficient measured for glass states, with respect to the equilibrium conditions, is represented in a more than satisfactory way, by the (NE) PC-SAFT model. It is worth noting that the latter is the output of a pure predictive calculation, based on the analysis of pure component equilibrium pVT properties and from a limited number of pure polymer out-of-equilibrium data, namely the glass transition temperature and the thermal expansion coefficient at the glassy state. The calculation was refined, in this case, through the further evaluation of the binary interaction coefficient, based on the analysis of solubility data at equilibrium conditions.

As for the purpose of this work, it is worth noticing that the results for the nonequilibrium infinite dilution solubility coefficient are obtained accounting for the peculiar condition in which the swelling coefficient is irrelevant to the calculation and the pseudoequilibrium polymer density is known, corresponding to the dry polymer glassy density. Under those conditions, indeed, the specific assumptions in the NE-RS model play no role in the calculation. The latter are essential, instead, in the determination of high-pressure gas or vapor solubility, and their role will be emphasized in the discussion of the two examples considered in the next subsection.

4.2. High-Pressure Gas and Vapor Solubility in Polycarbonate (PC). The case of sorption of CO_2 in PC is here considered first, for which the binary interaction parameter has been already retrieved in the previous subsection, from the analysis of true thermodynamic equilibrium solubility data. Application of the model in eq 3.2 requires that the value of the isothermal compressibility for the glassy polymeric phase $\kappa_{Tg}^{(g)}$ is first recognized, and the model parameter χ is finally estimated as the ratio between the compressibility for the glassy and melt phases at the transition point. The experimental pVT data for pure PC in Figure 3 are once more used to retrieve the value of $\kappa_{Tg}^{(g)} = 3.6 \times 10^{-4}\ MPa^{-1}$, and the corresponding estimate of model parameter χ for PC is reported in Table 2.

The high-pressure CO_2 content in PC, as predicted by the (NE-RS) PC-SAFT model at 35 °C, is here compared with experimental data measured by Fleming and Koros in ref 29. The comparison is illustrated in the plots reported in Figure 4. The good agreement between the pure prediction from the (NE-RS) PC-SAFT model and the high-pressure experimental data testifies to the capability of both the equilibrium and nonequilibrium models used.

https://doi.org/10.1021/acs.jced.3c00441
J. Chem. Eng. Data 2024, 69, 538−559

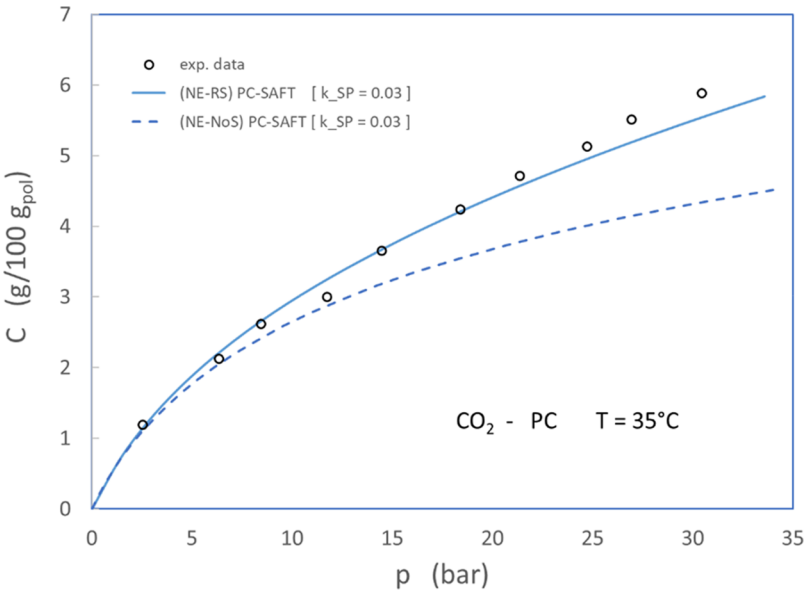

Figure 4. Analysis of high-pressure gas solubility data for CO_2 in PC; experimental data from ref 29.

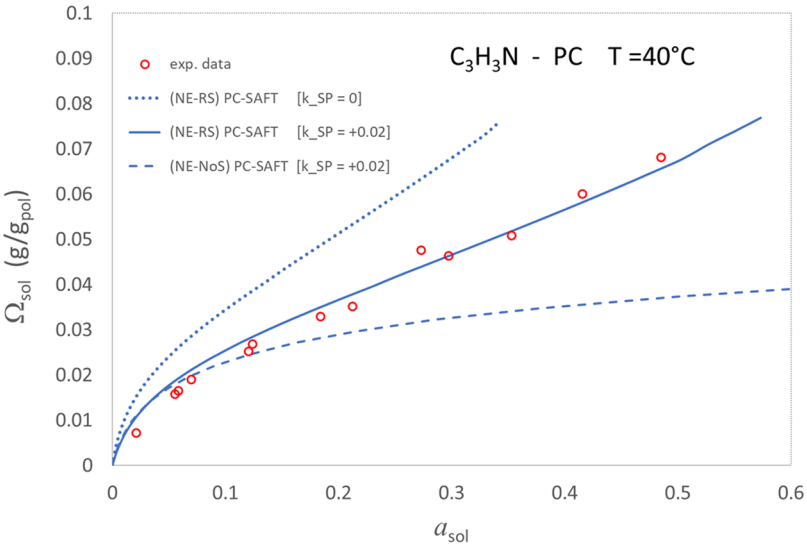

Figure 5. Analysis of vapor solubility data for acetonitrile in PC; experimental data from ref 30.

To emphasize the relevance and effect of the assumptions for volume swelling in the NE-RS model, in Figure 4, model results have also been reported for the case in which the sorption-induced volume swelling of the glassy polymer structure is ignored. Within the latter assumption, indicated in this work as the Nonequilibrium No Swelling (NE-NoS) model, the phase equilibrium problem is solved assuming that the pseudoequilibrium polymer density ρ_{pol}^{PE} is equal to the dry polymer density $\rho_{pol}^{0,PE}$ at the same temperature, at all pressure values.

From the data in Figure 4 it can be appreciated that a specific representation of sorption-induced volume swelling does not affect the infinite dilution solubility coefficient, as anticipated in the discussion in section 2 in this work, and its effect on the predicted solute content in glassy PC is indeed negligible up to a solute mass ratio of ~2%. The relevance of sorption-induced swelling in determining the pseudoequilibrium solute content becomes evident at larger concentration, and indeed, the data in the figure reveal that ignoring the phenomenon gives underestimates larger than 25% for the CO_2 content in PC at 35 °C, for pressure higher than 30 bar.

Accounting for sorption-induced volume swelling is then crucial for the description of vapor sorption at non-negligible activity, and as a result, interesting information can be retrieved from the analysis of volume dilation data in these cases. The best fit of solubility data measured for acetonitrile in PC, through the (NE-RS) PC-SAFT model, shown in Figure 5, will work as an example for that. Experimental data, reported in symbols, were measured by Giacinti Baschetti and co-workers,[30] and the calculated isotherm, reported as a solid blue line, was obtained by means of acetonitrile PC-SAFT parameters retrieved from the literature and using the binary interaction coefficient k_{sp} as the only adjustable parameter. The values for pure acetonitrile PC-SAFT parameters used in the calculation and the binary interaction coefficient retrieved from the procedure are indicated in Tables 1 and 3, respectively. The effect of the binary parameter in the model calculation can be appreciated

https://doi.org/10.1021/acs.jced.3c00441
J. Chem. Eng. Data 2024, 69, 538−559

Table 3. Binary Interaction Coefficient for Solute-PIM-1 Pairs Considered in the Calculations

substance	k_{SP} in PIM-1 (−)
H_2	0.000
N_2	0.000
O_2	0.000
CO_2	0.000
CH_4	0.000
C_2H_4	0.000
C_2H_6	0.000
C_3H_6	0.000
C_3H_8	0.000
n-heptane	0.000
toluene	0.000
DMC	0.000
methanol[a]	+0.020
ethanol[a]	+0.025
water[a]	−0.120

[a]Nonassociating model.

considering the comparison with prediction results for the default vale of k_{sp}, also shown in Figure 5.

It can be observed that the results from the model correlation satisfactorily represent the solubility coefficient S_{sol} in the entire pressure range, correctly interpreting the decrease of S by an order of magnitude from infinite dilution to 50% activity. The latter qualitative behavior is typical of gas/vapor sorption in glassy polymers, often described through the empirical Dual Mode model.[31] The relevance of accounting for sorption-induced volume swelling is also put in evidence, in Figure 5, through the comparison with results from the assumption of rigid polymer structure (NE-NoS) PC-SAFT. The analysis confirms that the contribution from volume swelling becomes dominant at larger solute activity values. It should also be noted that predictions for the case of nonswelling condition start departing from those obtained from the Restrained Swelling model just in the region where the solubility coefficient changes from the infinite dilution value to the high-activity value, corresponding to the "knee" in the isothermal solubility curve.

4.3. Volume Swelling Induced by Vapor Sorption Dilation. The analysis of experimental data for acetonitrile

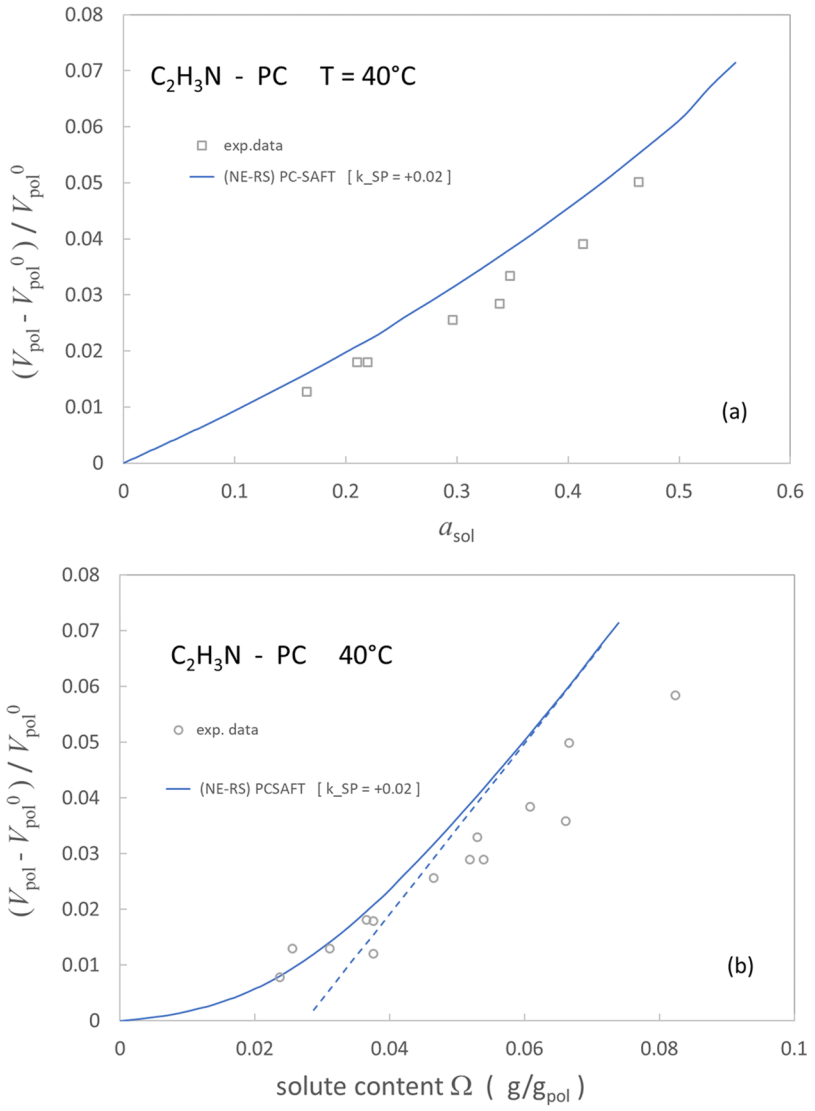

Figure 6. Sorption induced volume dilation in the acetonitrile-PC system at 40 °C: (a) system volume dilation vs activity; (b) system volume dilation vs solute content; experimental data from ref 30.

https://doi.org/10.1021/acs.jced.3c00441
J. Chem. Eng. Data 2024, 69, 538−559

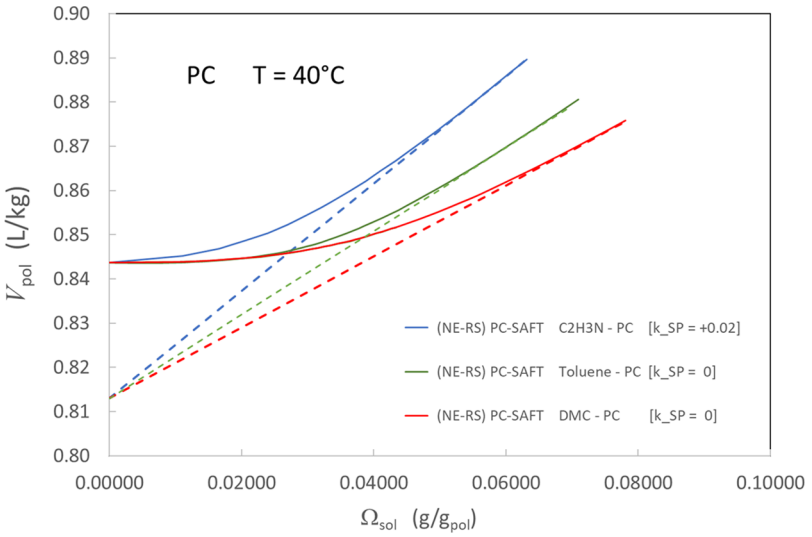

Figure 7. Analysis of the NE-RS model prediction of the sorption induced volume dilation in acetonitrile-PC, toluene-PC, and dimethyl carbonate-PC systems at 40 °C.

sorption in PC from the vapor phase, obtained by Giacinti, offers a very interesting opportunity for the objective of this work, as the authors also measured "in situ" the volume dilation of the polymer sample during the sorption experiment. A comparison is then in order between measured dilation and the prediction from the (NE_RS) PC-SAFT model, and this is presented in Figure 6. Results for changes in volume of the mixture are here represented through the variation of mixture volume per polymer mass V_{pol}. Plots in Figure 6a reveal that both experimental data and model results show a direct proportionality between volume dilation $\Delta V_{pol}/V_{pol}^{0}$ and solute activity a up to 40% activity, approximately, while predicted data show an upward trend for larger activity values. A linear increase of system volume with solute fugacity, from dry to significantly swollen conditions, is indeed typically observed for the gas/vapor sorption in glassy polymers and, upon observation of this general relation, empirical correlations for high-pressure solubility isotherms were proposed in early applications of the NET-GP model, based on the volume swelling coefficient.[32]

Also the analysis of volume dilation as a function of solute content is of interest in this discussion, and pertinent experimental data, as well as model predictions for acetonitrile-PC at 40 °C, are reported in Figure 6b. Data from model predictions show negligible values, at infinite dilution conditions, for the partial specific volume $\overline{V}_{sol}^{PE}$ of the solute component in the mixture, defined by the following relation

$$\overline{V}_{sol}^{PE} = \left(\frac{\partial V_{pol}}{\partial \Omega_{sol}}\right)_{T} \tag{4.2}$$

In turn, $\overline{V}_{sol}^{PE}$ increases when solute concentration increases, up to values of the same order of specific volume of the pure liquid solute component, although the equilibrium infinite dilution partial specific volume for the solute in the mixture would be a better reference in this case. This behavior, which is typical of sorption in a glassy polymer, hereafter will be referred to as "delayed volume dilation" in the sorption condition, and the x-axis intercept of the high solute content linear trend for $\overline{V}_{sol}^{PE}$ may be taken as a measurement of the magnitude of the "delay".

The qualitative trend returned by the model prediction for $\overline{V}_{sol}^{PE}$ as a function of Ω_{sol} is confirmed by experimental data in Figure 6b, although the swelling coefficient at the asymptotic limit in measured dilation is lower than the corresponding value from model predictions, and the same is true for the magnitude of the dilation "delay".

The (NE-RS) PC-SAFT model interpretation of the variation of V_{pol} with solute concentration is indeed rather interesting, as illustrated in Figure 7, where model predictions for the case of sorption of acetonitrile in PC at 40 °C are compared with those predicted for toluene (TOL) and dimethyl carbonate (DMC) sorption. Model prediction results for the volume dilation induced by sorption of DMC or TOL in PC have been obtained for the default value of the binary interaction parameter ($k_{sp} = 0$). It is interesting to mention, however, that model predictions obtained for different values of k_{sp} in the range from −0.1 to +0.1 confirm that results for volume dilation as a function of solute mass ratio in the (NE-RS) model are substantially independent of the binary interaction parameter. The dashed lines in Figure 7 represent the tangent lines to the V_{pol} curve, in the region where the solute partial specific volume has reached a constant value. The slopes of the dashed lines for C_2H_3N, toluene, and DMC are measured as 1.21, 0.95, and 0.80 L/kg, respectively, to be compared with the saturated pure liquid specific volumes calculated by PC-SAFT as 1.22 L/kg for C_2H_3N, 1.18 L/kg for TOL, and 0.97 L/kg for DMC at 40 °C. As it can be appreciated from the plot, the high concentration limit trend for V_{pol} intersects the y-axis (dry polymer conditions) at the same value for all solute components considered and, noticeably, this value corresponds to the "equilibrium" value for the pure polymer specific volume as predicted by the EoS (see data in Figure 3). The latter should be regarded as an empirical observation about the results from the NE-RS model, and it offers the opportunity of a simple model-driven interpretation of solubility results. In fact, the positive difference between the actual pure polymer specific volume (y-axis intercept of the solid curves in Figure 7) and the "equilibrium" value (y-axis intercept of the dashed curves in Figure 7) corresponds to the excess free volume in the glassy polymer phase. For the case of PC at 40 °C, the excess free volume counts approximately 3%, both by the data in Figure 3 and by those in Figure 7. Relying on the latter model interpretation, experimental data for volume dilation at sorption conditions in a glassy polymer could be used, in

https://doi.org/10.1021/acs.jced.3c00441
J. Chem. Eng. Data 2024, 69, 538−559

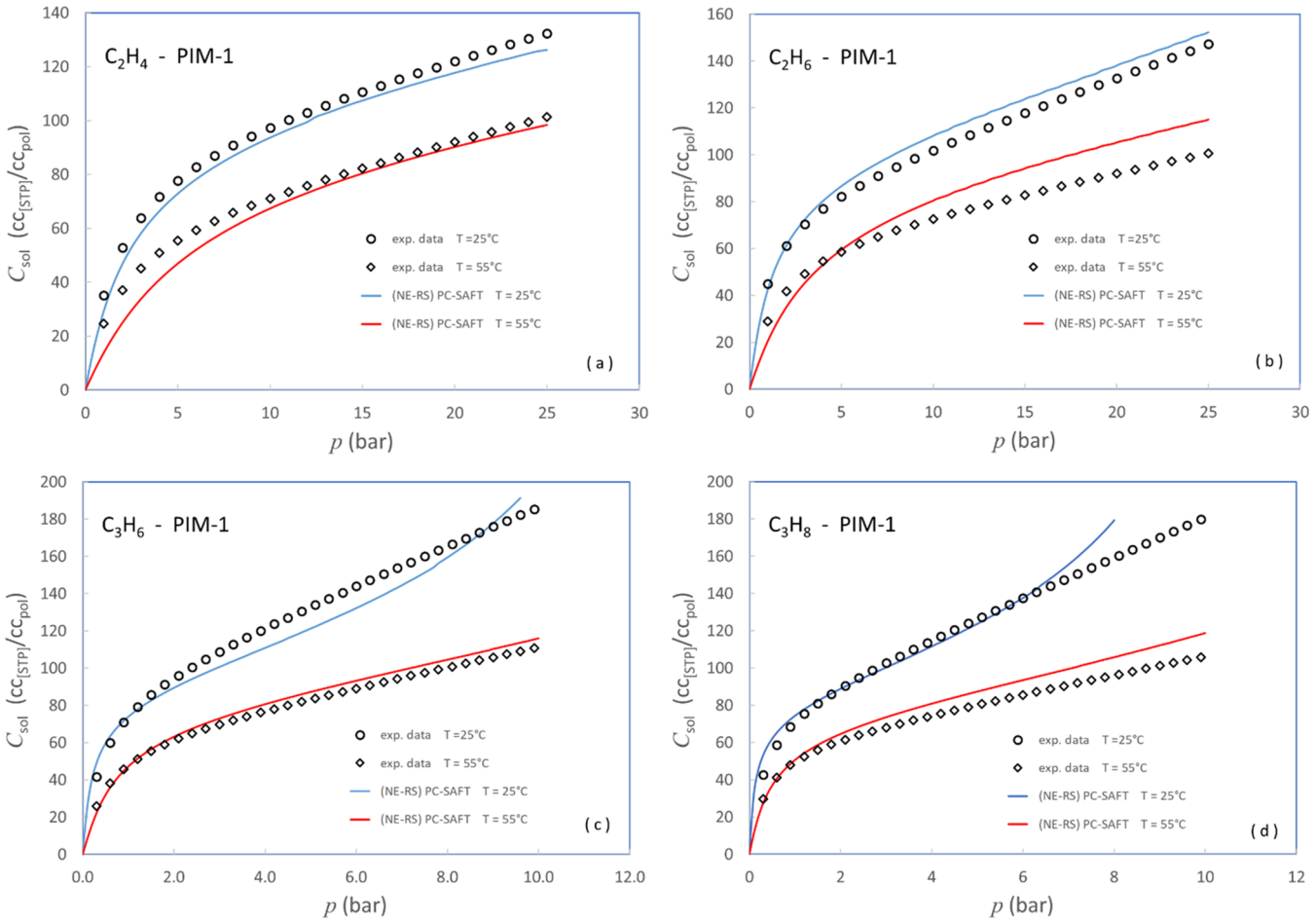

Figure 8. Results from the best fit of high-pressure alkane gas sorption in PIM-1: (a) ethylene-PC; (b) ethane-PC; (c) propylene-PC; (d) propane-PC. Experimental data from ref 36.

principle, to estimate the equilibrium specific volume of the pure polymeric species, at the same temperature, not directly accessible through experimental techniques. Unfortunately, measurements of volume dilation at sorption conditions are complex to take, and reliable values for this kind of data are rare in the literature.

At the end of this section it is finally mentioned that, while results have been here reported for the first applications of the PC-SAFT EoS to the NE-RS model representation of pseudoequilibrium glassy properties, the robustness and physical significance of the NE-RS model are shown in the numerous analyses of solubility and volume swelling performed in previous papers, in which the cases of several different penetrant-polymer pairs and those of different sample pretreatments were examined, based on the representation of the equilibrium properties provided by the Sanchez−Lacombe lattice fluid model.[17,18]

5. ANALYSIS OF VAPOR SOLUBILITY IN A POLYMER WITH INTRINSIC MICROPOROSITY (PIM-1)

A different case is examined in this section, referring to a polymeric material for which neither equilibrium nor non-equilibrium volumetric data are available in a reliable form. Experimental data are here considered for gas and vapor solubility in the first material synthesized within the class of "Polymers with Intrinsic Microporosity" (PIM-1).[33] The latter corresponds to a polymeric species with a very rigid backbone structure, which prevents the system from efficiently packing and which is, indeed, accredited to an exceptionally high free volume fraction, at room temperature. Its glass transition point cannot be measured directly, as its value exceeds the degradation temperature for the material, although indirect measurements have been attempted recently, which indicate an approximate value of 644 °C.[34,35] We can thus classify PIM-1 as a "superglassy" polymer, whose characteristics are more than appealing for gas and vapor separation through membrane processes, as the high-free-volume structure allows for high gas/vapor solubility and diffusivity coefficient. On the other hand, the density of PIM-1 samples, as well as solubility properties, largely depends on the preparation protocol and sample pretreatment. In addition to that, the same properties typically change over time, according to environmental conditions, through physical aging processes. The unattainability of the equilibrium melt phase and the variability of results from density measurements at room conditions, of course, make it impossible to replicate the procedure illustrated in the previous section for the case of conventional glassy polymers.

5.1. Retrieval of (NE-RS) PC-SAFT Model Parameters for PIM-1. The model analysis of the solubility characteristics of PIM-1 may be indeed only pursued by selecting a series of data measured in sorption experiments from different gases and vapors and looking for the best fit of results in relatively large temperature and pressure intervals, through the adjustment of all unknown model parameters in the problem described by eq 3.2.

https://doi.org/10.1021/acs.jced.3c00441
J. Chem. Eng. Data 2024, 69, 538−559

The latter list, on the other hand, includes the EoS parameters for PIM-1, glass transition temperature, glassy state thermal expansion coefficient, and isothermal compressibility, as well as binary interaction coefficients for each solute considered in the set of selected solubility data.

Optimal representation of the parameters in the process described above may be a hard objective to achieve, when the search is not carefully guided. In the present work, as for the retrieval of pure PIM-1 model parameters, high-pressure solubility data from hydrocarbon vapors have been chosen, among numerous results presented in the literature. It may be assumed that the binary interaction coefficients in PIM-1 for components in the same class are similar, thus reducing the number of unknowns in the problem. Data reported by Li for the solubility of ethylene, ethane, propylene, and propane, at two different temperatures,[36] have thus been selected to this aim. In order to facilitated the search for the best fit of the solubility data modeled through (NE-RS) PC-SAFT in eq 3.2, the thermal expansion coefficient for glassy PIM-1 is preliminary assumed here as $\alpha_{T_g}^{(g)} = 2.0 \times 10^{-4}\ K^{-1}$, corresponding to the value which characterizes most conventional glassy polymeric materials, although the value for superglassy polymers may often depart from it.[26,34,35] The pure component PC-SAFT solute parameters considered in the calculations are taken from the literature and listed in Table 1.

It must be mentioned that, in the work by Li, experimental data for solubility are reported as solute molar content per unit volume of dry polymer. In model calculations, the latter quantity is independent from the mass of polymer hard spheres $(M/m)^{(\text{PIM-1})}$ and, thus, the best fit procedure for the selected data has been performed by adjusting the parameters in the following list: PIM-1 glass transition temperature $T_g^{(\text{PIM-1})}$, ratio between glassy and melt isothermal compressibility $\chi^{(\text{PIM-1})}$, PIM-1 hard sphere diameter $\sigma^{(\text{PIM-1})}$, PIM-1 characteristic interaction energy $\varepsilon^{(\text{PIM-1})}$, solute-PIM-1 binary interaction parameter k_{sp}, assumed to have just the same, temperature independent value, for all solutes in the class of aliphatic alkanes. The solubility isotherms resulting from the best fit procedure are shown in Figure 8, while the values of the model parameters retrieved for PIM-1 are listed in Table 1, for the case of PC-SAFT pure component parameters and in Table 2 for what is referred to as specific nonequilibrium NE-RS parameters. In Table 3, finally, indication is given that the best fit results were obtained from the default mixing rule for the nonhomogeneous interaction energy in alkane-(PIM-1) systems, accounting for the null value of the binary interaction parameter k_{sp} in eq 2.11 for all alkane components.

The identified set of parameters allowed us to obtain an acceptable representation of vapor solubility isotherms from low to high pressure, described by the average deviations reported in Table 4, for the calculated solute fugacity at the assigned temperature and concentration, with respect to the corresponding experimental data. Beyond the value of the average deviation for fugacity, it clearly results from plots in Figure 8 that the retrieved parameters allow for a correct representation of the temperature effect on solubility for all gases considered, as well as for the ratio between the low-pressure and high-pressure solubility coefficients. The absolute value of the infinite dilution solubility coefficient is also represented in a satisfactory way in the series of data considered, with the exception of the high-temperature ethylene sorption isotherm, for which the model result is one-third lower than the experimental value. It must be observed, however, that the solubility coefficient is significantly overpredicted by the (NE-RS) PC-SAFT model for the case of the highest solute mass ratio in the series of data analyzed, corresponding to low-temperature, high-pressure propane and propylene sorption. In fact, the model prediction of the solute content seems to diverge from the experimental results for the case of very high solute fugacity. The latter results indicate that the model predicts a nonlinear increase of volume with solute fugacity at the highest solute content which fails to match experimental results for the case of solute volume ratio larger than 50%, while the qualitative trend and quantitative results appear adherent to the experimental value for the lower solute volume fraction in the system. Finally, it should also be noted that the specific NE-RS model parameter compressibility ratio χ, as determined for PIM-1 from the best fit procedure in this analysis, is significantly higher than that experimentally measured for conventional glassy polymers.[17]

Table 4. Average Deviation of Model Predictions from Experimental Data, for Alkane Gas Solute Fugacity in PIM-1 versus Solute Concentration at Different Temperature Values[a]

	AAD	
	T = 25 °C	T = 55 °C
C_2H_4	13%	14%
C_2H_6	14%	24%
C_3H_6	17%	11%
C_3H_8	9%	21%

[a]As obtained from the best fit procedure in which equilibrium and nonequilibrium volumetric properties of polymeric species have been used as adjustable parameters.

5.2. Prediction of Infinite Dilution Gas Solubility and Sorption Enthalpy in PIM-1. In the work by Li, solubility data are also reported for the case of permanent gases in PIM-1.[36] Similar to the case of vapors, experimental data are reported in terms of molar content per dry polymer volume, measured at different temperatures, around room conditions. For each gaseous species considered, the infinite dilution solubility coefficient at 35 °C and the corresponding sorption enthalpy can be retrieved from the experimental data reported. Comparison was then considered between the data for $S_0^{35\,°C}$ and $\Delta\tilde{H}_0$ as estimated from the experimental results and those obtained from the application of the (NE) PC-SAFT model, through a pure predictive procedure (see data in Table 5). For the sake of discussion of the consistency of the model predictions, it should be considered that the experimental data for sorption enthalpy are affected by a larger error, with respect to the solubility coefficient data, as the first are numerically

Table 5. Comparison between Experimental Data and Model Pure Predictions for the Infinite Dilution Solubility Coefficient and Heat of Sorption in PIM-1[a]

	$S_0^{35\,°C}$ $(cc_{[STP]}/cc_{pol}\ bar)$			$[-\Delta H_0]$ (kJ/mol)		
		model results			model results	
	exp data	(NE) PC-SAFT	EoS PC-SAFT	exp data	(NE) PC-SAFT	EoS PC-SAFT
N_2	2.4	2.0	0.11	+14	+13	−1.7
O_2	3.1	2.7	0.23	+21	+13	+0.9
CH_4	8.2	4.7	0.33	+19	+15	+2.4
CO_2	35.0	21.0	2.5	+22	+23	+12

[a]Experimental data from ref 36.

https://doi.org/10.1021/acs.jced.3c00441
J. Chem. Eng. Data 2024, 69, 538−559

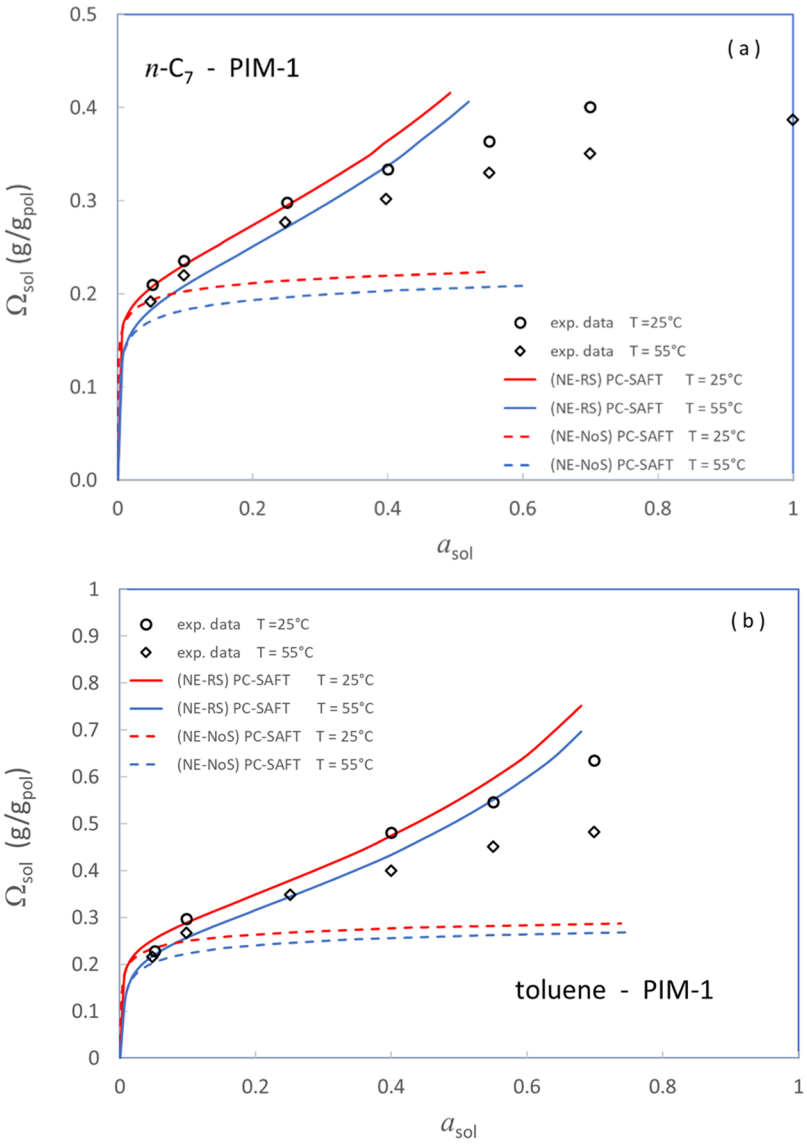

Figure 9. Results from experimental data and model prediction of the vapor solute content as a function of activity in PIM-1 at two different temperatures: (a) *n*-heptane-PIM-1 system; (b) toluene-PIM-1 system; experimental data from ref 20.

evaluated from the sensitivity of the latter to temperature after eq 4.1.

For the procedure of model prediction of the solubility coefficient and sorption enthalpy, PC-SAFT parameters for gaseous species were retrieved from the literature and reported in Table 1, while all binary interaction parameters were set to the default null value, in model calculations. Results from model predictions well compare with experimental data, although the model slightly underestimates the solubility coefficient in all cases, and the sorption enthalpy in a few. In Table 5, results are also reported for the infinity dilution solubility coefficient and sorption enthalpy as calculated for the corresponding equilibrium polymer structure, after the use of the same set of model parameters. It can be appreciated that results from the equilibrium EoS lie an order of magnitude below the corresponding experimental and nonequilibrium model results. It can also be observed that, for the case of nitrogen sorption in PIM-1, the equilibrium EoS describes the sorption as a weak endothermic process, opposite to the strong exothermic nature revealed by the experimental data and confirmed by the NET-GP calculation.

5.3. Prediction of Vapor Solubility in PIM-1. The PIM-1 model parameters retrieved in the procedure reported above have then been tested with reference to the analysis of further vapor solubility data for heptane and toluene, for which DGRPT model correlations have been already compared with data measured at high activity values, at two different temperatures.[20] It must be stressed that, different from the case of the experimental results discussed earlier, the data for *n*-heptane and toluene solubility considered in this procedure are reported in terms of solute mass content per polymer mass, in the system. In the calculation of this specific quantity from the (NE-RS) PC-SAFT model in eq 3.2, the mass of the PIM-1 hard sphere $(M/m)^{(\mathrm{PIM\text{-}1})}$ is relevant, and the latter parameter has been then here adjusted to the best fit of these experimental data, accounting again for the null value of the binary interaction parameter for both hydrocarbon species in PIM-1. It should be first noted that the solubility coefficient S_{sol} cannot be quantitatively retrieved from available experimental data, in the limit of infinite dilution,

https://doi.org/10.1021/acs.jced.3c00441
J. Chem. Eng. Data 2024, 69, 538−559

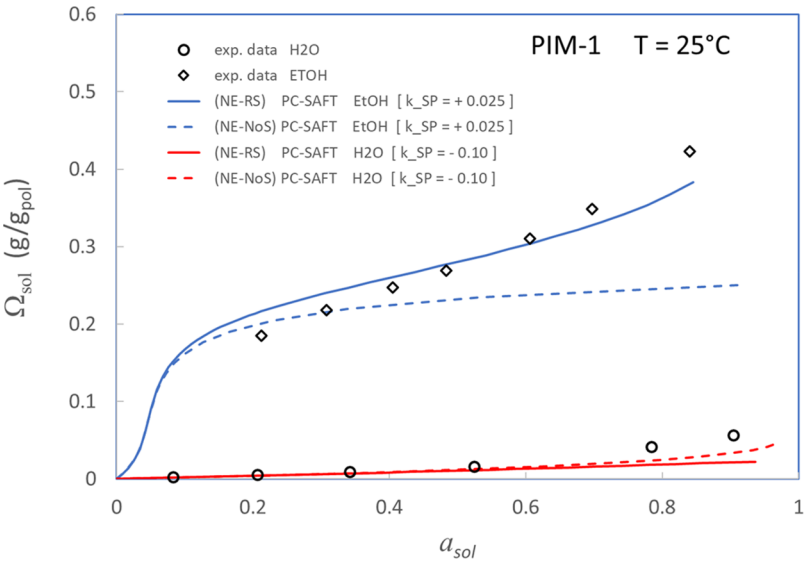

Figure 10. Results from the experimental data and model prediction of solute content as a function of activity for ethanol and water sorption in PIM-1. Experimental data from ref 37.

but it clearly results that S_{sol} rapidly decreases by orders of magnitude, as the solute content exceeds a threshold value on the order of 20%. From plots in Figure 9 it can be noticed that changes in the solubility coefficient of both *n*-heptane and toluene are correctly represented by the model, also in terms of the temperature effect, at least for the case of low and moderate vapor activity, while the model overestimates the swelling of the system at activity higher than 0.4. The value of the EoS model parameter $(m/M)^{(\mathrm{PIM\text{-}1})}$ retrieved in this procedure is reported in Table 1.

In the same figures, results are also reported for the solubility isotherm predicted by the NET-GP model, obtained after the assumption of the nonswelling polymer matrix [(NE-NoS) PC-SAFT]. In all cases considered, the results from this assumption are consistent with measured data, in the terms indicated in the previous section, as they give account of the experimental evidence for S_{sol} up to the threshold value for the solute content at which the solubility coefficient rapidly decreases. The comparison between the results from Restrained Swelling and nonswelling allow us to conclude that the (NE-RS) model correctly predicts the volume swelling induced by sorption up to about 40% activity, for both toluene and *n*-heptane, roughly corresponding to 30−40% mass uptake, in the two cases. It can also be deduced that, like the case of propane and propylene examined above, the (NE-RS) PC-SAFT model set up in this work for PIM-1 predicts a nonlinear volume swelling with solute fugacity, at higher solute content, corresponding again to the volume ratio on the order of 50%, which is not reported in the experimental evidence.

Data for the vapor solubility of the non-hydrocarbon species in PIM-1 were also considered in this work, specifically referring to the case of dimethyl carbonate (DMC), water, methanol, and ethanol. It should be first considered that the latter species are typically interpreted as associating components in the PC-SAFT representation of thermodynamic properties. More specifically, water and alcohols are described as self-associating, while DMC is described as prone to induced association. This is a relevant issue, as also PIM-1, whose chemical structure includes ether groups in the backbone, may be considered as subject to induced association phenomena. On the other hand, for the description of this specific aspect, at least two additional model parameters (association energy and characteristic volume) should be included in the discussion and optimized, based on the best fit of the solubility data of the associating components in PIM-1. Following the criterion adopted also for the previous comparison, and looking for a description of the thermodynamic properties which is based on the lowest possible number of adjustable parameters, the choice has been taken in this work to model the thermodynamic properties of all mixtures through the PC-SAFT EoS, without specifically accounting for hydrogen bonding and considering only the dispersion term for the representation of interactions in all systems. Through this choice, the prediction of the solubility data in PIM-1 could be discussed in terms of one binary interaction coefficient only, for each solute-polymer pair. To this aim, the mass, diameter, and characteristic energy of the hard sphere in each vapor component were first determined, based on the best fit of vapor pressure and saturated liquid density as a function of temperature. Indeed, a satisfactory representation of the vapor−liquid equilibrium conditions was obtained for water, methanol, ethanol, and DMC, and the PC-SAFT model parameters retrieved this way are reported in Table 1. Results from the best fit of the saturated vapor properties within the scheme of the nonassociating components for water, methanol, ethanol, and DMC are reported in the Supporting Information. It should be here mentioned that the same approach was attempted also for propanol and butanol, for which more solubility data in PIM-1 were available. However, the best representation of vapor pressure and saturated liquid density which could be obtained for these heavier alcohol species, through the nonassociating scheme, was not satisfactory enough to be included in the same group with the components mentioned above.

The plots in Figure 10 compare the experimental and model results for ethanol and water solubility in PIM-1 at 25 °C. An acceptable representation of ethanol sorption in PIM-1 was obtained, after the binary interaction parameter was adjusted to a moderate positive value, while the (NE-RS) model predicts negligible pseudoequilibrium solute content for water in PIM-1 and a value close to those measured in experiments could be represented only accounting for relevant negative values of k_{sp}.

https://doi.org/10.1021/acs.jced.3c00441
J. Chem. Eng. Data 2024, 69, 538−559

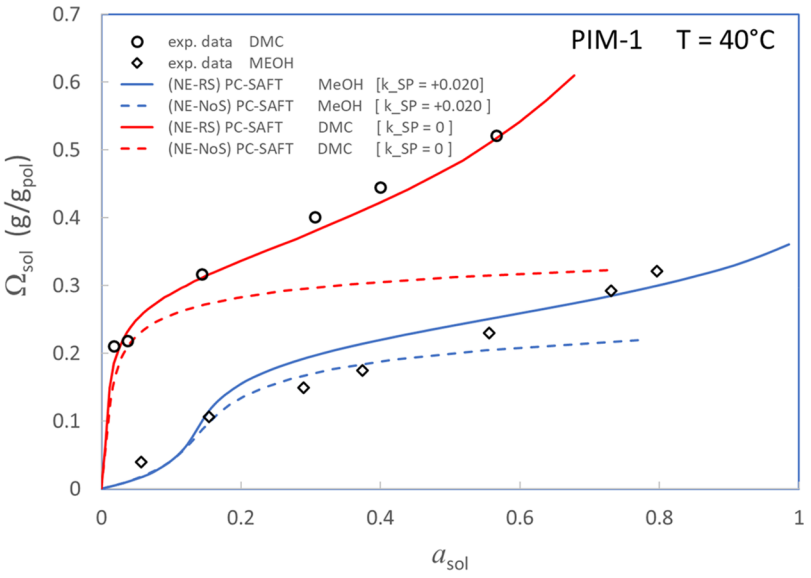

Figure 11. Results from experimental data and model prediction of solute content as a function of activity for DMC and methanol sorption in PIM-1. Experimental data from ref 38.

The binary interaction coefficients retrieved in the above procedure are all reported in Table 5. It can also be observed that the (NE-RS) PC-SAFT model predicts a complex S-shaped isotherm at low contents of ethanol, in which the solubility coefficient shows a maximum value for relatively low solute content. The low activity behavior predicted by the model is the result of the difference in characteristic energy of the homogeneous interaction in PIM-1 and in ethanol. As for the comparison with predictions obtained ignoring the sorption-induced volume dilation [(NE-NoS) PC-SAFT], also shown in Figure 10, it can be noticed that the data for ethanol show the same features already observed for alkane sorption in PIM-1, with a contribution from volume swelling which well compares with experimental results in average terms, although the sensitivity of solute fugacity to composition appears over-estimated in model predictions with respect to experimental data. For the case of water, on the other hand, comparison between NE-RS and NE-NoS results reveals that, in this case, a moderate increase in volume results in a moderate increase in solute fugacity, at fixed concentration and temperature, opposite to the results observed for all remaining solute species.

In Figure 11, model predictions are finally compared with experimental data for the solubility of methanol (MeOH) and dimethyl carbonate (DMC) in PIM-1 at 40 °C measured by Cihal.[38] It can be noticed that DMC sorption is more than satisfactorily represented in the whole activity range in which experimental data are available, without the need of adjusting the value of the binary interaction parameter ($k_{sp} = 0$). An acceptable representation was obtained also for methanol solubility, after the binary interaction parameter was adjusted to a moderate positive value ($k_{sp} = +0.02$). Also in this case, the model results for the assumption of a rigid polymer matrix [(NE-NoS) PC-SAFT] are consistent with the low-activity experimental results, while the contribution from sorption-induced volume swelling looks relevant at solute mass ratios larger than 20% for DMC and larger than 10% for methanol.

6. DISCUSSION

Model representation of gas/vapor solubility data in superglassy polymers is a severe challenge in many respects, starting from variability of polymer sample pseudoequilibrium properties with the specific preparation protocol used. Unattainability of melt conditions for the pure polymer prevents the possibility to directly measure equilibrium pVT polymer properties and to tailor the corresponding EoS model through the same univocal procedure used for conventional polymers. For the case of PIM-1, also glassy pVT data are scarce in the literature and unreliable, again in view of their general variability with the preparation protocol and of changes induced by aging phenomena.

The polymer parameters required to set up a (NE-RS) PC-SAFT model were then retrieved in section 5.1, through the best fit of low- and high-pressure gas and vapor solubility data of alkanes in PIM-1, after the assumption that the thermal expansion coefficient in the glassy state is similar to the typical value shown by conventional polymers.

The results obtained in this procedure indicate a glass transition temperature for PIM-1 which is significantly lower than the values most accredited in the literature, and also the thermal expansion coefficient value used does not find confirmation in results from direct characterization of thermal properties.[35] The room temperature dry polymer density returned by the properties retrieved in the procedure, equal to 1.021 *kg/L*, is within the range of rather different values reported in the literature. On the other hand, the experimental data available for that are spread in an interval which is too large for the comparison to be significant, within the NET-GP model, in which relatively small differences in dry polymer mass density may result in rather different values for gas or vapor solubility.

Equilibrium and out-of-equilibrium pure PIM-1 properties retrieved through the procedure were then used to predict the infinite dilution solubility coefficient and sorption enthalpy for light gases in PIM-1, as well as solubility isotherms at different temperatures, in a large activity range, for several vapors. Appreciable and consistent results were then obtained in model prediction of gas and vapor solubility up to moderate activity, including the representation of remarkably high values of infinite dilution solubility coefficient for vapors and that of the dramatic change of S_{sol} with solute content.

Comparison of complete model results with calculation performed assuming a null value of volume swelling show that

https://doi.org/10.1021/acs.jced.3c00441
J. Chem. Eng. Data 2024, 69, 538−559

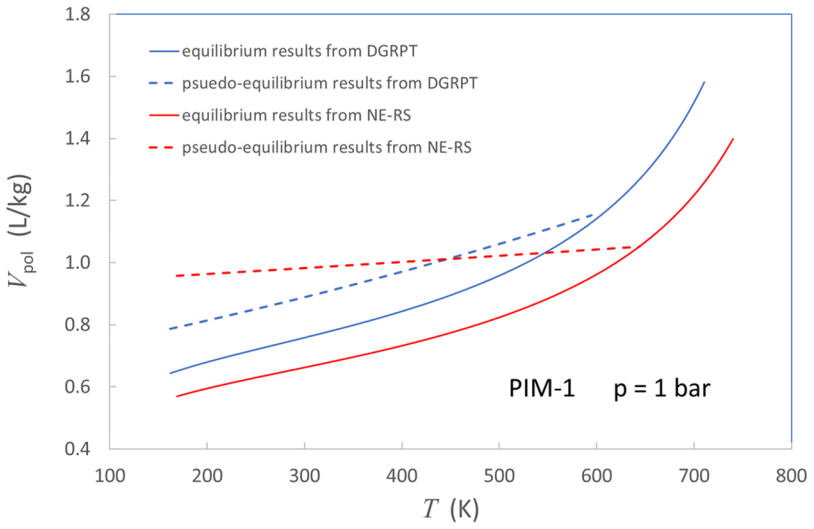

Figure 12. Comparison of equilibrium and pseudoequilibrium low-pressure specific volume for PIM-1 as retrieved from (NET-GP) PC-SAFT analysis of vapor solubility data according to the NE-RS and DGRPT models.

the (NE-RS) PC-SAFT model set up for PIM-1 in this work correctly predicts the sorption-induced swelling coefficient at low and moderate solute concentrations. In almost all examples considered, however, the model predicts a sorption-induced volume dilation which increases more than proportionally to the solute fugacity at high solute concentration, which ultimately results in overpredictions of vapor solubility at solute content larger than 50% by volume, in all cases examined.

It should be noted that, with respect to the assumption of direct proportionality between volume dilation and solute fugacity made in previous implementations of the NET-GP model, in which the swelling coefficient was used as the binary adjustable parameter,[32] the NE-RS model here considered represents a predictive procedure and it extends naturally to the case of mixed gas or vapor sorption. The reason for the highly nonlinear volume swelling predicted by the model could lie in the extreme value of the nonequilibrium properties of PIM-1 retrieved from the best fit procedure of alkane solubility and specifically in the unusually high value of glassy isothermal compressibility, with respect to the case of conventional polymers analyzed so far in the same model framework. The latter argument suggests the use of a larger and more variegate set of solubility data for the retrieval of the equilibrium and nonequilibrium pVT properties of pure PIM-1, and this kind of analysis will be considered in future works.

The comparison is now in order of results from the analysis performed in this work, with that offered by Marshall for the vapor solubility in PIM-1,[20] through the use of alternative route DGRPT, for closure of the phase equilibrium problem in the NET-GP approach. Although, in the work by Marshall, several experimental data sets were analyzed among those considered in the present work, direct comparison of the average deviation in solute fugacity of the predicted solubility would not be significant, as very different databases, criteria, and strategies were used, in the two analyses, for the retrieval of the same model parameters. It is first mentioned here that, as a result of the best fit procedure, the solubility isotherms in DMC, heptane, toluene, and several alcohols were satisfactorily described at different temperatures through the DGRPT model, in the entire activity range explored by experimental data, while water sorption was significantly overestimated.

A direct comparison is possible, on the other hand, of equilibrium and nonequilibrium pVT properties for PIM-1 retrieved in the two analyses, which indeed represent the actual output of the best fit procedures performed in both cases. The procedure performed by Marshall and co-workers led to a characteristic interaction energy $(\varepsilon/k)_p = 176\ K$, which is very close to that retrieved in this work. The latter conditions ensure that the low-pressure equilibrium thermal expansion coefficient α^0 values for PIM-1 predicted by the two models are very close, one to the other, at all temperatures [see function $\alpha^0(T) = \frac{1}{T}Y\left(\frac{kT}{\varepsilon}\right)$ in the Supporting Information]. As also the hard sphere diameter retrieved in ref 20, equal to $\sigma_p = 2.78\ Å$, is not far from that obtained in this work, it results that the low-pressure compressibility κ^0 values predicted by the two models are less that 20% apart, at any temperature (see function $\kappa^0(T) = \frac{5\pi\sigma^3}{24\varepsilon}X\left(\frac{kT}{\varepsilon}\right)$ in the Supporting Information). On the other hand, the absolute value of the equilibrium specific volume is rather different in the PC-SAFT models for PIM-1 obtained from NE-RS and DGRPT analysis of vapor solubility data, in view of the different value retrieved for hard sphere mass ($m/M = 0.0468\ mol/g$ in ref 20.). The same is true for the thermal expansion coefficient in the glassy state ($\alpha^{(g)} = 8.8 \times 10^{-4}\ K^{-1}$ in ref 20), while the PIM-1 pVT properties returned by DGRPT analysis are consistent with the glass transition temperature values obtained in this work (T_g = 610 K for parameters retrieved in ref 20).

In Figure 12 results are compared for equilibrium, as well as nonequilibrium, the low-pressure specific volume of PIM-1 as retrieved from NE-RS and DGRPT analysis of vapor solubility data, both accounting for the PC-SAFT EoS representation of equilibrium properties within the NET-GP approach.

It is interesting to observe that, while the specific volume values for dry PIM-1 at room temperature retrieved in the two procedures (dashed lines in Figure 12) are similar, the corresponding value for the "excess free volume", equal to the distance between the dashed line and solid line in Figure 12, is rather different. The value resulting from the DGRPT analysis, indeed, is approximately one-half of that retrieved in the present work.

https://doi.org/10.1021/acs.jced.3c00441
J. Chem. Eng. Data 2024, 69, 538−559

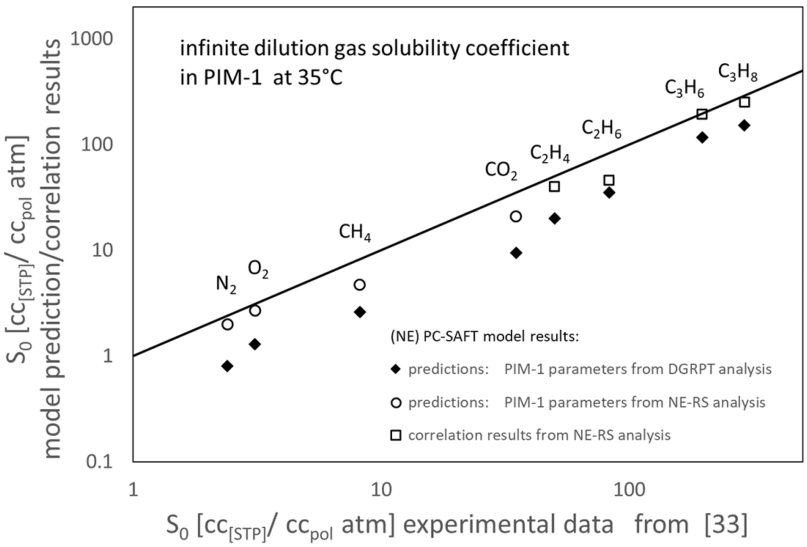

Figure 13. Parity plot for the infinite dilution solubility coefficient of different gases in PIM-1 at 35 °C; comparison between experimental data from ref 33 and (NE) PC-SAFT model results, both from the set of PIM-1 pure component model parameters retrieved in this work and from that derived in ref 20.

A straightforward comparative analysis of consistency for pure PIM-1 volumetric properties represented in Figure 2, and retrieved in the two procedures, can be managed by the discussion of the gas solubility coefficient, resulting from the use of the two different sets of parameters, through the NET-GP model. It has been clarified in section 2, in fact, that for the calculation of $S_0^{NET\text{-}GP}$, only EoS parameters and the dry polymer density are needed, while the procedure used to account for solvent-induced volume dilation has no role. In Figure 13, results are then compared for S_0 calculated in PIM-1 at 35 °C from the set of model parameters retrieved in this work, and from the alternative set obtained in ref 20 after the analysis of vapor sorption in PIM-1 through the DGRPT model. Model results from both sets of parameters, all obtained accounting for the default null value of the binary interaction parameter for gases in PIM-1, are compared with the experimental data reported in ref 33, for several gases. In the open symbols, results from the first set of parameters are reported, in which pure prediction data for light gases are distinguished from those for alkanes, which took part in the procedure for the retrieval of model parameters and are thus indicated as "correlation" data. In the same figure, pure prediction results from the use of the second set of model parameters are represented in filled symbols, and both are compared with experimental data in the parity-plot diagram. Predictions from both sets of PIM-1 pure component parameters underpredict the infinite dilution solubility coefficient for all gases. The average deviation from experimental data for results from the two formulations of pure PIM-1 pVT properties, however, is rather different. Indeed, while the accuracy of predictions from the use of parameters retrieved from the present NE-RS analysis of high-pressure gas solubility data is about 20%, the infinite dilution gas solubility coefficient calculated after the set of parameters returned by the DGRPT analysis of vapor solubility data is less than half the corresponding experimental value, in almost all cases. The difference in prediction from the two sets of model parameters appears to be strictly related to the difference in the excess free volume described by the distinct volumetric properties shown in Figure 12. Indeed, the extremely large infinite dilution gas solubility coefficient measured in PIM-1 is consistently represented as driven by the mixing entropy in the NE-RS analysis here discussed, ultimately resulting from the very large excess volume of the dry polymer matrix. The same data, on the other hand, could only be represented through the set of PIM-1 parameters retrieved in the DGRPT analysis, by accounting for an extremely high excess mixing enthalpy, expressed, in all cases, through the more than significant negative value of the gas-polymer binary interaction parameter (not calculated here).

Further interesting indications can be derived by extending the above comparison between model calculations after swelling and no-swelling assumptions to the results from DGRPT analysis of vapor sorption in PIM-1. For the sake of comparison with NE-RS predictions shown in Figure 9, results are reported in Figure 14 as obtained from the correlation performed in ref 20 for the solubility data of *n*-heptane and toluene in PIM-1, at different temperatures. It can be observed that results from DGRPT analysis (solid lines in figure), in which the binary interaction coefficient k_{sp} in PIM-1 has been set to −0.0445 and +0.0107 for *n*-heptane and toluene, respectively, are qualitatively different from those retrieved from the pure prediction performed in this work after the NE-RS approach. Indeed, the solubility coefficient returned by the DGRPT correlation is a decreasing function of solute content for both components, and overall, it well compares with experimental data in the full activity range.

The difference in sorption induced volume swelling represented through the DGRPT model, with respect to NE-RS, is in evidence when results are considered as calculated from the assumption of the nonswelling polymer matrix, for the set of PC-SAFT model parameters and PIM-1 dry glassy density retrieved in ref 20. The latter results, which have been calculated in this work, are shown in dashed lines in Figure 14. When compared with the corresponding results in Figure 9, it can be appreciated that the high-activity limiting value of the solute content calculated from the NE-NoS approach, in this case, is less than half the value obtained when the PIM-1 parameters retrieved in this work are considered, for both solutes. This is the neat effect of the different excess volumes predicted for dry PIM-1 by the two sets of parameters and represented in Figure 12. On the other hand, a remarkable difference is in evidence between

https://doi.org/10.1021/acs.jced.3c00441
J. Chem. Eng. Data 2024, 69, 538−559

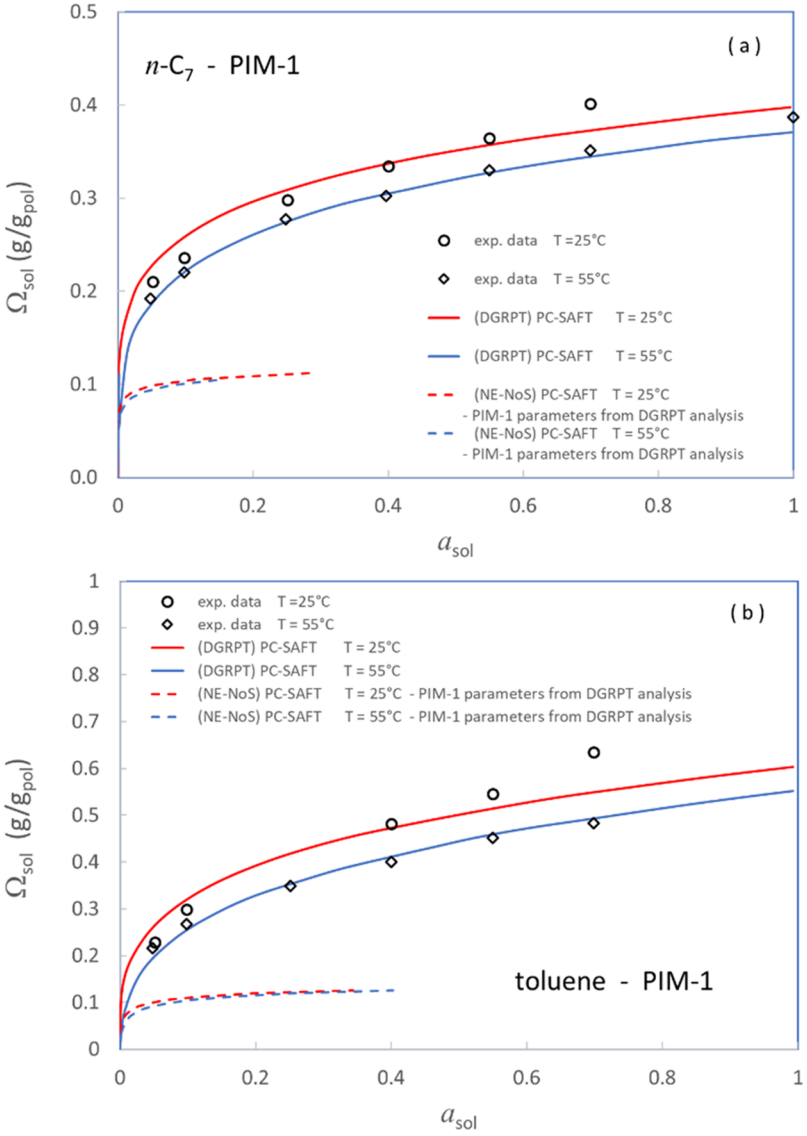

Figure 14. Experimental data and DGRPT model results for the analysis of vapor solute content as a function of activity in PIM-1 at different temperatures: (a) *n*-heptane-PIM-1 system; (b) toluene-PIM-1 system; experimental data and (DGRPT) PC-SAFT results from ref 20.

the data in solid and dashed lines in Figure 14, at low activity values, when compared with the corresponding data in Figure 9. The latter result testifies the much larger contribution from the volume dilation to the low-fugacity solute content in DGRPT than in the NE-RS model, and it should be attributed to the significant differences in the general description of sorption-induced volume swelling used in the two approaches.

A specific comparison of volumetric behavior described by the two different closure assumptions for the NET-GP model can be managed considering their descriptions of phase equilibrium conditions in methanol-(PIM-1) and in DMC-(PIM-1) mixtures, as the "in situ" experimental data of sorption-induced volume dilation were measured by Cihal[38] for the two systems.

In Figure 15 experimental data are compared with the predictions from the two models in terms of system dilation vs activity. The substantial proportionality relation between volume dilation and solute pressure is confirmed in the experimental data, while the NE-RS model predictions again exhibit an upward trend with increasing volume dilation. More significant, however, is the fact that the volume dilation predicted by the NE-RS model is approximately one-third of the value measured experimentally, both in the case of methanol and in that of DMC sorption. In the same figure, also results for sorption-induced volume dilation obtained through DGRPT are reported and it can be easily observed that the trends described by the two models are opposite. In the DGRPT description of phase equilibrium conditions, in fact, the volume dilation coefficient is larger, in average terms, with respect to the experimental data, and it decreases with solute activity. The latter trend of swelling coefficient is emphasized in model results for the DMC-(PIM-1) system.

It can be said that rather similar results for the vapor solubility in PIM-1 are given in the two approaches, at least for the cases of low and moderate activity values, with DGRPT accounting for a significantly lower excess free volume of dry polymer phase and much larger sorption-induced volume dilation, with respect to NE-RS.

Additional insights in the dilation mechanism predicted by the two models are obtained when the predicted volume dilation is discussed as a function of solute content in the mixture, according to the general argument presented in Section 4.3, for the analysis of sorption-induced volume dilation in conventional

https://doi.org/10.1021/acs.jced.3c00441
J. Chem. Eng. Data 2024, 69, 538−559

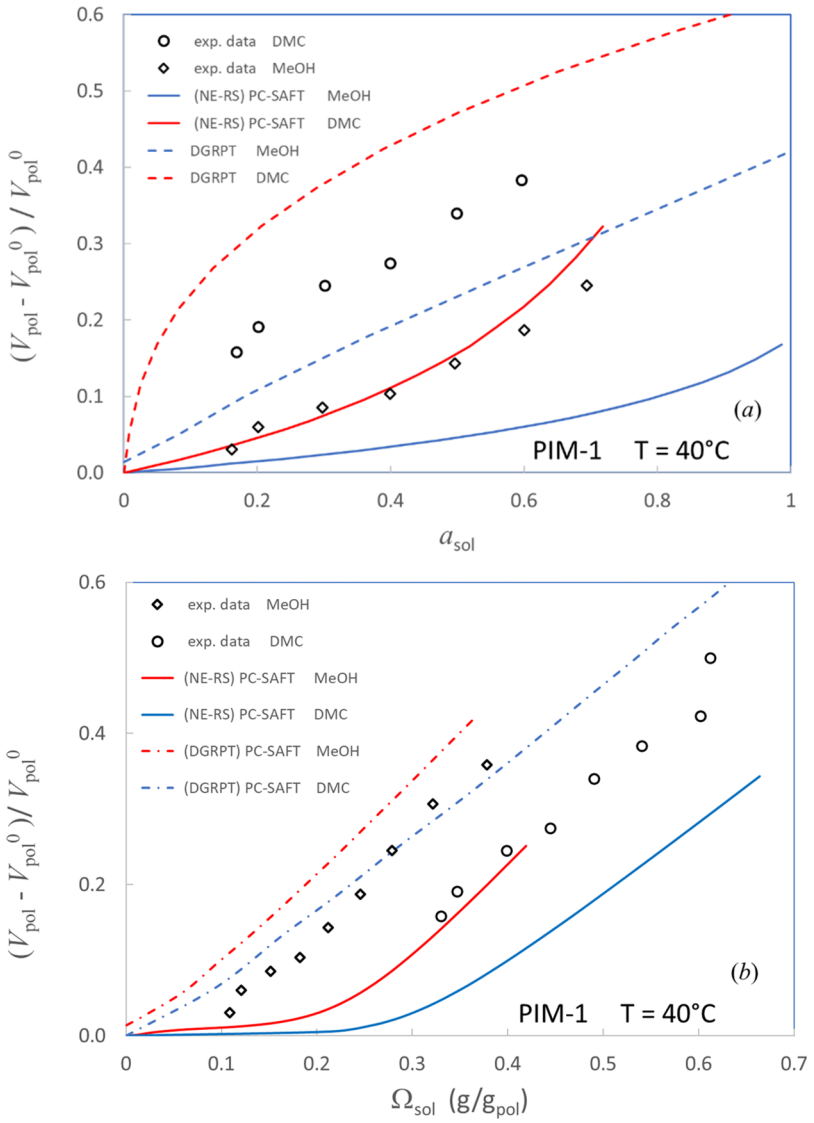

Figure 15. Sorption-induced volume dilation in the DMC-(PIM-1) and methanol-(PIM-1) systems at 40 °C; experimental data from ref 38; DGRPT results from ref 20: (a) system volume dilation vs solute activity; (b) system volume dilation vs solute content.

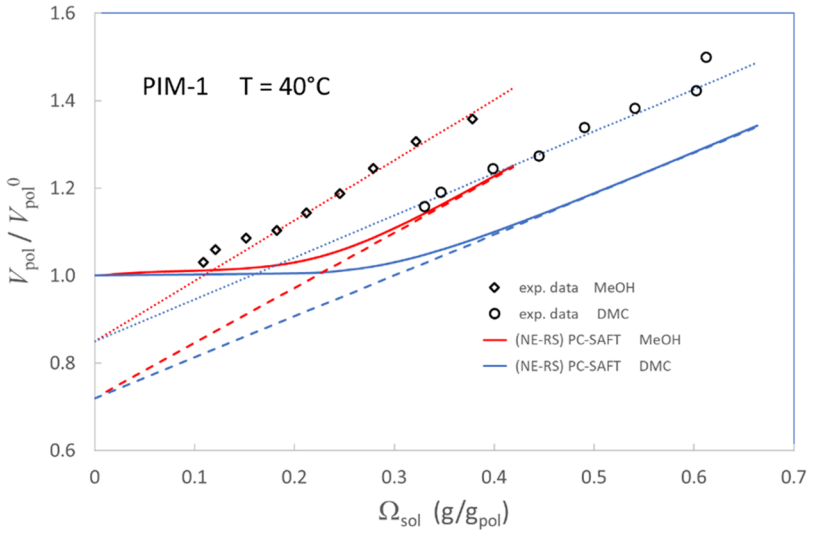

Figure 16. Analysis of sorption-induced volume dilation in the DMC-(PIM-1) and methanol-(PIM-1) systems at 40 °C; experimental data from ref 38.

https://doi.org/10.1021/acs.jced.3c00441
J. Chem. Eng. Data 2024, 69, 538−559

glassy polymers. Data for the relative volume variation in the system, as a function of solute content, are reported in Figure 15b, as calculated from the two models, and compared with pertinent experimental data by Cihal.[38] Interestingly, the models offer two rather different results for the partial specific volume as a function of solute content. The NE-RS model predicts a negligible value of the solute partial specific volume $\overline{V}_{sol}^{PE}$ at infinite dilution, both for the methanol-(PIM-1) and DMC-(PIM-1) systems, while the value rapidly increases, in the two cases, when the solute mass ratio exceeds 20%, and it finally reaches a constant value at higher solute content, in the order of equilibrium pure solute specific volume. The DGRPT model, instead, only shows limited variation of the partial specific volume over the mass ratio in both systems examined, and no "delay" is shown by the volume dilation predicted in this approach with respect to the mass uptake in the systems. For the case of either the methanol-(PIM-1) or DMC-(PIM-1) system, the experimental data show results which are intermediate between those of the two models here discussed. A delay in dilation, with respect to the mass uptake, is actually evident in the experimental data, but its magnitude appears to be significantly smaller than that predicted by the NE-RS approach.

It must be concluded that the criteria implemented for the sorption-induced volume dilation in the two models are rather different. The differences, however, are somehow hidden in the examination of the predicted solubility data, as an ultimately reasonable comparison with the same experimental data is obtained from both approaches when different swelling criteria are combined with different values of dry polymer excess volume.

A comment is finally due about the comparison between the "delayed dilation" phenomenon in PIM-1, as described by the experimental data and predicted by NE-RS model. The comparison will be managed through the model-driven analysis proposed in the previous section. From the plot in Figure 16, it can be appreciated that the asymptotic linear relation between V_{sol} and Ω_{sol} is registered at high solute content both in the NE-RS model and in the experimental results. It can also be observed that, for each solute separately, the slope of the asymptotic trend is substantially the same in the experimental data and model prediction. On the other hand, the y-axis intercept of the asymptotic linear trend, common to curves pertinent to different solutes, appears significantly higher in the experimental data than in the model prediction. As in the model interpretation the intercept identifies the expected true equilibrium value of the volume in the pure polymer phase, the conclusion can be drawn that the excess free volume shown by experimental results (15%) is almost half the value considered in the (NE-RS) PC-SAFT model set up in this work for PIM-1. It should also be observed that the value for the excess free volume derived from the proposed analysis of the experimental data is close to that returned by the set of PIM-1 parameters retrieved in the DGRPT procedure (see data in Figure 12).

It is clear from the above analysis that the two approaches to the description of sorption-induced volume dilation are not equivalent, and rather different results are expected from the use of the NE-RS and DGRPT models, when the same values are considered for the volumetric properties of polymeric species. The analysis performed in this work represents a nonconclusive contribution to the discussion of the capabilities of the two approaches, in view of the limited number of systems considered for the comparison. The discussion offered here, however, clarifies the qualitative differences between the descriptions of volume swelling returned by the two closure conditions for the NET-GP approach proposed in the NE-RS and DGRPT models.

7. CONCLUSIONS

The relevance of pure polymer pVT properties, for both melt and glassy phases, in the determination of gas and vapor solubility below the glass transition temperature has been elucidated in this work, through the use of the Nonequilibrium Restrained Swelling (NE-RS) model, implemented with the PC-SAFT representation of equilibrium properties.

Cases are distinguished, in this analysis, of conventional and superglassy polymers. In the first case, the mass density, isothermal compressibility, and thermal expansion coefficient are available, both above and below the glass transition temperature T_g and, under these conditions, gas or vapor solubility can be estimated, based on essentially predictive procedures, at all temperatures. In the opposite case, gas/vapor solubility data as a function of temperature and solute fugacity can be used to retrieve equilibrium and nonequilibrium pure polymer volumetric properties.

A few examples of the first kind of analysis have been presented in this work, also discussing a straightforward procedure to retrieve PC-SAFT model parameters from polymer pVT data, for the limiting case of infinite molecular mass of polymeric species.

The case of a polymer with intrinsic microporosity (PIM-1) has been here considered as an example of the second kind of analysis, and its pure component PC-SAFT parameters, as well as glassy volumetric properties, have been determined based on the best fit of the solubility results for a series of gas/vapor hydrocarbon species. The equilibrium and nonequilibrium volumetric properties of PIM-1 derived in the procedure were then compared with those retrieved, in a similar analysis, from the use of the DGRPT approach to the closure on the NET-GP problem for the phase equilibrium solution in polymer solvent systems. The two approaches ultimately account for similar equilibrium properties, but for rather different values of excess free volume for the dry polymer, and definitely different sorption-induced volume dilations.

A model driven analysis of the experimental data for sorption-induced volume dilation has been presented, which is oriented to the direct evaluation of the excess free volume of dry glassy polymer. The results from the analysis of the available corresponding data for DMC and MeOH sorption in PIM-1 are consistent with the polymer excess free volume resulting in the DGRPT analysis by Marshall et al.[20]

The analysis of a larger set of experimental results, including the case of conventional glassy polymers, and of the corresponding predictions from both the NE-RS and DGRPT approaches would be required to make conclusions about the reliability of solute-induced volume dilation predicted in the two models and to identify possible routes to further improve the capability of the general NET-GP model.

■ ASSOCIATED CONTENT

Supporting Information

The Supporting Information is available free of charge at https://pubs.acs.org/doi/10.1021/acs.jced.3c00441.

S.I: General procedure for retrieving pure component PC-SAFT parameters for nonassociating, high-molecular-weight species after low-pressure pVT data. S.II:

https://doi.org/10.1021/acs.jced.3c00441
J. Chem. Eng. Data 2024, 69, 538−559

Procedures for the solution of equilibrium and pseudoequilibrium problems in this work. S.III: Figures with best fit results for vapor pressure and saturated liquid density of water, ethanal, methanol, and dimethyl carbonate as obtained in this work from PC-SAFT EoS for nonassociating components and tables reporting numerical results for model calculations shown by plots in the figures in the main body of the manuscript (PDF)

AUTHOR INFORMATION

Corresponding Author

Ferruccio Doghieri − *Department of Civil, Chemical, Materials and Environmental Engineering, University of Bologna, I-40131 Bologna, Italy;* orcid.org/0000-0002-6140-2324; Email: ferruccio.doghieri@unibo.it

Complete contact information is available at: https://pubs.acs.org/10.1021/acs.jced.3c00441

Notes

The author declares no competing financial interest.

NOTATION

a_{sol}	solute activity
C_{sol}	solute molar concentration in solute-polymer mixture
f_{sol}	solute fugacity
$f_{sol}^{(G)}$	solute fugacity in gas phase
f_{sol}^{PE}	solute fugacity value at pseudoequilbrium condition
f_{sol}^{EQ}	equilibrium solute fugacity function in solute-polymer mixture (see eq 2.1)
k	Boltzmann constant
k_{sp}	binary interaction coefficient
m_p, m_s	number of hard spheres per molecule in polymer/solute (PC-SAFT model parameter)
M_p, M_s	molecular mass of polymer/solute species
p	pressure
$p^{0,EQ}$	equilibrium function for pressure in pure polymer
S_{sol}	solute solubility coefficient in the polymer-solute mixture
$S_{0,sol}$	infinite dilution solubility coefficient
T	temperature
T_g	glass transition temperature
V	specific volume of the system
V^0	low-pressure specific volume
V_{pol}	system volume per polymer mass (= $1/\rho_{pol}$)
V_{pol}^0	dry polymer specific volume
$\overline{V}_{sol}^{PE}$	solute partial specific volume in polymer solute mixture (see eq 4.2)
Y ()	universal PC-SAFT equation defined in eq S.7 and reported in Table S1
X ()	universal PC-SAFT equation defined in eq S.12 and reported in Table S1
$\alpha^{(g)}$	dry polymer thermal expansion coefficient at glassy state
$\alpha_{Tg}^{(g)}$	dry polymer glassy thermal expansion coefficient at glass transition
$\alpha_{Tg}^{(m)}$	dry polymer melt thermal expansion coefficient at glass transition
$\Delta\tilde{H}_{0,sol}$	infinite dilution solute sorption enthalpy in solute-polymer mixture (see eq 4.1)
ε_p, ε_s	characteristic interaction energy for polymer/solute species (PC-SAFT parameter)
ε_{sp}	characteristic energy for polymer/solute interaction
$\kappa^{(g)}$	dry polymer isothermal compressibility at glassy state
$\kappa_{Tg}^{(m)}$	dry polymer melt isothermal compressibility at glass transition
κ_Ω	sorption-induced volume swelling coefficient in the solute polymer mixture (see eq 2.3)
ρ_{pol}	polymer mass density (polymer mass per system volume)
ρ_{pol}^{PE}	pseudoequilbrium polymer mass density
$\rho_{pol}^{0,PE}$	pseudoequilbrium dry polymer mass density
ρ_{sol}	solute mass density (solute mass per system volume)
ρ_{Tg}	polymer mass density at glass transition temperature
σ_p, σ_s	polymer/solute hard sphere diameter (PC-SAFT model parameter)
χ	glassy to melt compressibility ratio (see eq 3.1)
Ω_{sol}	solute mass ratio in solute-polymer mixture

REFERENCES

(1) Wang, Y. G.; Ghanem, B. S.; Ali, Z.; Hazazi, K.; Han, Y.; Pinnau, I. Recent Progress on Polymers of Intrinsic Microporosity and Thermally Modified Analogue Materials for Membrane-Based Fluid Separations. *Small Structures* **2021**, *2*, No. 2100049.

(2) Golubev, G. C.; Volkov, V. V.; Borisov, I. L.; Volkov, A. V. High free volume polymers for pervaporation. *Current Opinion in Chemical Engineering* **2022**, *36*, No. 100788.

(3) Kirchheim, R. Partial Molar Volume of Small Molecules in Glassy-Polymers. *J. Polym. Sci. Polym. Phys.* **1993**, *31*, 1373−1382.

(4) Ricci, E.; De Angelis, M. G. Modelling Mixed-Gas Sorption in Glassy Polymers for CO2 Removal: A Sensitivity Analysis of the Dual Model Sorption Model. *Membranes* **2019**, *9*, 8.

(5) Vopicka, O.; Friess, K. Analysis of Gas Sorption in Glassy Polymers with the GAB Model: An Alternative to Dual Mode Sorption Model. *J. Polym. Sci. Polym. Phys.* **2014**, *52*, 1490−1495.

(6) Mensitieri, G.; Scherillo, G.; Panayiotou, C.; Musto, P. Towards a predictive thermodynamic description of sorption processes n polymers: The synergy between theoretical EoS models and vibrational spectroscopy. *Mater. Sci. Eng. R-Rep.* **2020**, *140*, No. 100525.

(7) Doghieri, F.; Sarti, G. C. Nonequilibrium lattice fluids: A predictive model for the solubility in glassy polymers. *Macromolecules.* **1996**, *29*, 7885−7896.

(8) Sanchez, I. C.; Lacombe, R. H. An Elementary Molecular Theory of Classical Fluids. Pure Fluids. *J. Phys. Chem.* **1976**, *80*, 2352−2362.

(9) Lacombe, R. H.; Sanchez, I. C. Statistical thermodynamics of fluid mixtures. *J. Phys. Chem.* **1976**, *80*, 2568−2580.

(10) Doghieri, F.; Sarti, G. C. Predicting the low pressure solubility of gases and vapors in glassy polymers by the NELF model. *J. Membr. Sci.* **1998**, *147*, 73−86.

(11) Doghieri, F.; Ghedini, M.; Quinzi, M.; Rethwish, D.; Sarti, G. C. Predicting gas solubility in glassy polymers through Non-Equilibrium eos. *Abstract of Papers of The American Chemical Society* **2001**, *222*, U363.

(12) Minelli, M.; Doghieri, F. A Predictive Model for Vapor Solubility and Volume Dilation in Glassy Polymers. *Ind. Eng. Chem. Res.* **2012**, *51*, 16505−16516.

(13) Marshall, B.; Mathias, R.; Lively, R. P.; McCool, B. A. Theoretically Self-Consistent Nonequilibrium Thermodynamics of Glassy Polymer Theory for the Solubility of Vapors and Liquids in Glassy Polymers. *Ind. Eng. Chem. Res.* **2021**, *60* (36), 13377.

(14) Mathias, R.; Weber, D. J.; Thompson, K. A.; Marshall, B. D.; Finn, M. G.; Scott, J. K.; Lively, R. P. Framework for predicting the fractionation of complex liquid feeds via polymer membranes. *J. Membr. Sci.* **2021**, *640*, No. 119767.

(15) Marshall, B. D.; Allen, J. W.; Lively, R. P. A model for the separation of complex liquid mixtures with glassy polymer membranes: A thermodynamic perspective. *J. Membr. Sci.* **2022**, *647*, No. 120316.

(16) Marshall, B. D.; Li, W.; Lively, R. P. Dry Glass Reference Perturbation Theory Predictions of the Temperature and Pressure

Dependent Separations of Complex Liquid Mixtures Using SBAD-1 Glassy Polymer Membranes. *Membranes* **2022**, *12*, 705.
(17) Minelli, M.; Doghieri, F. Predictive model for gas and vapor solubility and swelling in glassy polymers I: Application to different polymer/penetrant systems. *Fluid Phase Equilib.* **2014**, *381*, 1−11.
(18) Minelli, M.; Doghieri, F. Predictive model for gas and vapor solubility and swelling in glassy polymers: II. Effect of sample previous history. *Fluid Phase Equilib.* **2017**, *444*, 47−55.
(19) Astarita, G. *Thermodynamics: An advanced textbook for Chemical Engineers*; Plenum: New York (NY-USA), 1989.
(20) Marshall, B. D.; Johnson, J. R. Dry glass reference perturbation theory predictions of the pervaporation separation of solvent mixtures using PIM-1 membranes. *J. Membr. Sci.* **2023**, *672*, No. 121420.
(21) Gross, J.; Sadowski, G. Perturbed-Chain SAFT: An Equation of State Based on a Perturbation Theory for Chain Molecules. *Ind. Eng. Chem. Res.* **2001**, *40*, 1244−1260.
(22) Gross, J.; Sadowski, G. Application of the perturbed-chain SAFT equation of state to associating systems. *Ind. Eng. Chem. Res.* **2002**, *41*, 5510−5515.
(23) Wang, J.-S.; Kamiya, Y. Evaluation of Gas Sorption Parameters and Prediction of Sorption Isotherms in Glassy Polymrs. *J. Polym. Sci. Polym. Phys.* **2000**, *38*, 883−888.
(24) Tumakaka, F.; Gross, J.; Sadowski, G. Modeling of polymer phase equilibria using Perturbed-Chain SAFT. *Fluid Phase Equilib.* **2002**, *194*, 541−551.
(25) Zoller, P.; Walsh, D. A. *Standard Pressure-Vol.-Temperature Data for Polymers*; Technomic: Lancaster (PA-USA), 1995.
(26) Ghosh, A.; Chapman, W. G.; French, R. N. Gas solubility in hydrocarbons − a SAFT-based approach. *Fluid Phase Equilib.* **2003**, *209*, 229−243.
(27) Pokorny, V.; Stejfa, V.; Fulem, M.; Cervinka, C.; Ruzicka, K. Vapor Pressures and Thermophysical Properties of Dimethyl Carbonate, Diethyl Carbonate and Dipropyl Carbonate. *J. Chem. Eng. Data* **2017**, *62*, 3206−3215.
(28) Perry, R. H.; Green, D. W. *Perry's Chemical Engineering Handbook*, VII ed.; Mc Graw Hill: New York (NY-USA), 1997.
(29) Fleming, G. K.; Koros, W. J. Dilation of Polymers by Sorption of Carbon Dioxide at Elevated Pressures. 1 Silicon Rubber and Unconditioned Polycarbonate. *Macromolecules* **1986**, *19*, 2285−2291.
(30) Giacinti Baschetti, M.; Piccinini, E.; Barbari, T. A.; Sarti, G. C. Quantitative Analysis of Polymer Dilation during Sorption Using FTIR-ATR Spectroscopy. *Macromolecules* **2003**, *36*, 9574−9584.
(31) Paul, D. R. Fundamentals of transport phenomena in polymer membranes. In *Comprehensive membrane science and engineering*; Drioli, E, Giorno, L, Eds.; Academic: Oxford, 2010; Vol *1*, pp 75−90.
(32) Baschetti, M. G.; Doghieri, F.; Sarti, G. C. Solubility in Glassy Polymers: Correlations through the Non-Equilibrium Lattice Fluid Model. *Ind. Eng. Chem. Res.* **2001**, *40* (14), 3027−3037.
(33) Li, P.; Chung, T. S.; Paul, D. R. Gas sorption and permeation in PIM-1. *J. Membr. Sci.* **2013**, *432*, 50−57.
(34) Yamato, M.; Imai, A.; Kawakami, H. Thermal properties of polymer with intrinsic microporosity membranes. *Polymer* **2022**, *259*, No. 125339.
(35) Yin, H.; Chua, Y. Z.; Yang, B.; Schick, C.; Harrison, W. J.; Budd, P. M.; Boehning, M.; Shönhals, A. First Clear-Cut Experimental Evidence of a Glass Transition in a Polymer with Intrinsic Microporosity. *J. Phys. Chem. Lett.* **2018**, *9*, 2003−2008.
(36) Li, P.; Chung, T. S.; Paul, D. R. Temperature dependence of gas sorption and permeation in PIM-1. *J. Membr. Sci.* **2014**, *450*, 380−388.
(37) Vopicka, O.; Friess, K.; Hynek, V.; Sysel, P.; Zgazar, M.; Sipek, M.; Pilnacek, K.; Lanc, M.; Jansen, J. C.; Mason, C. R.; Budd, P. M. Equilibrium and Transient sorption of vapours and gases in the polymer of intrinsic microporosity PIM-1. *J. Membr. Sci.* **2013**, *434*, 148−160.
(38) Cihal, P.; Vopicka, O.; Durdakova, T.-M.; Budd, P. M.; Harrison, W.; Friess, K. Pervaporation and vapor permeation od methanol-dimethyl carbonate mixtures through PIM-1 membranes. *Sep. Pur. Technol.* **2019**, *217*, 206−214.
(39) Kleiner, M.; Gross, J. An equation of state contribution for polar components: Polarizable dipoles. *AIChE J.* **2006**, *52*, 1951−1961.

https://doi.org/10.1021/acs.jced.3c00441
J. Chem. Eng. Data 2024, 69, 538−559